DEVELOPING NEW TECHNIQUES AND MATERIALS TO USE IN BIOSENSORS FOR POINT-OF-CARE APPLICATIONS

A Thesis

Presented to the Faculty of the Graduate School

of Cornell University

In Partial Fulfillment of the Requirements for the Degree of

Master of Science

by

Sarah Jessica Reinholt

January 2014

ABSTRACT

Biosensor technology is a rapidly expanding field of study in which tedious culturing techniques are being replaced by assays that use biorecognition elements such as antibodies and nucleic acids to detect biological entities. Biosensors have useful applications in areas such as food safety, water quality, clinical analysis, and defense again bioterrorism. Bench-top macro scale detection assays have limitations that restrict them to laboratory settings and require them to be performed by highly-trained personnel. Consequently, there has been a strong emphasis on developing technology that is portable and easy-to-use to enable its use in point-of-care and resource-limited settings. Thus, the concept of a micro total analysis system (μTAS) in which all aspects of the biological assay are contained within a single device is very attractive. Benefits of μTASs over their macro scale counterparts, aside from portability and increased ease-of-use, include smaller sample sizes, reduced reagent consumption, decreased assay time, negligible contamination, and potential automation.

Nucleic acid detection within μTASs is a commonly used method for the detection of cells and other microorganisms, as well as genomic analyses. A critical step in these assays is nucleic acid isolation within the microfluidic device. Miniaturizing nucleic acid isolation has led to the discovery of novel isolation techniques. Specific application and assay parameters determine desired characteristics of an optimal nucleic acid purification technique. Relevant parameters include sample type and size, device material and fabrication technologies available, as well as the pre- and post-isolation processes. The main nucleic acid isolation processes used within microfluidic devices are silica-based surfaces, functionalized paramagnetic beads, oligonucleotide-modified polymer surfaces, pH-dependent charged surfaces, aluminum oxide membranes, and liquid-phase isolation.

A common process that follows isolation is nucleic acid amplification, and integrating both steps within the same device is key to developing a complete μTAS. Nucleic acid sequence-based amplification (NASBA) is an isothermal amplification technique of which the primary advantage over the standard polymerase chain reaction (PCR) is the elimination of necessary thermal cycles. In this research, nucleic acid isolation and NASBA were integrated within the same simple microchannel to realize highly sensitive detection of very low concentrations of messenger RNA (mRNA). The microchannels were fabricated simply and inexpensively from poly(methyl methacrylate) (PMMA) using hot-embossing and UV/ozone-assisted thermal bonding. Unique surface chemistry modifications, involving the immobilization of polyamidoamine (PAMAM) dendrimers and subsequent covalent attachment of thymidine oligonucleotide probes to the dendrimer periphery, were used to develop a surface to facilitate the capture of mRNA from *Cryptosporidium parvum* (*C. parvum*) oocyst lysate, while remaining a suitable surface for NASBA. Using this very simple device, successful mRNA isolation and NASBA-based amplification from as few as 30 *C. parvum* oocysts was achieved.

An emerging area of point-of-care biosensor technology is that of paper-based sensors, and specifically, the lateral flow assay (LFA) has been very well-established. The main advantages of these types of sensors are that they are inexpensive, small, portable, disposable, easy-to-use, and require no external equipment or power source due to their capillary wicking ability. Traditionally, these biosensors are fabricated from cellulose-based fibers, which have fixed properties and limited chemical modification ability. Here, electrospun nanofibers have been presented as a new material for LFAs, since their properties are highly controllable and there are numerous materials from which the nanofibers can be made, giving countless surface modification possibilities.

Poly(lactic acid) (PLA)-based nanofibers were optimized and incorporated into LFAs. Initial experiments demonstrated a successful one-step assay in which streptavidin-coated sulforhodamine B (SRB)-encapsulating liposomes were captured by anti-streptavidin antibodies adsorbed onto the nanofiber surface. Subsequently, an enzymatic sandwich immunoassay was developed for *Escherichia coli* (*E. coli*), and a limit of detection of $1.9x10^4$ cells was achieved. Finally, functional polymers were used to demonstrate that the notorious problem of non-specific binding can be eliminated through the use of anti-fouling block copolymers. Functionalized electrospun nanofibers can thus be used to enhance paper-based assays and develop highly sensitive and specific biosensors possessing many significant advantages compared to traditional assays.

Concluding from the microfluidic and LFA research presented, point-of-care biosensors can be developed in a variety of formats, each having their own benefits and limitations. By catering the characteristics of the assay to the parameters surrounding its application, an ideal, reliable biosensor can be realized.

BIOGRAPHICAL SKETCH

Sarah Reinholt is originally from Sarnia, Ontario, Canada. She graduated with a Bachelor of Applied Science in Nanotechnology Engineering from the University of Waterloo in Waterloo, Ontario, Canada in 2011. Her undergraduate degree was a cooperative program in which she had workterms at Baylis Medical Company, Xerox Research Centre of Canada, and Cornell University. She joined the Baeumner Lab in the Department of Biological and Environmental Engineering in the College of Agriculture and Life Sciences at Cornell University in Fall 2011. In her spare time, Sarah enjoys playing ice hockey and softball as well as other athletics.

To my parents, Tim and Heather Reinholt, for their enduring love and support.

ACKNOWLEDGMENTS

I would like to express my most sincere gratitude to the Chair of my Special Committee, Dr. Antje Baeumner, for her incredible support throughout my Master's Degree. I could not have completed this work without her terrific guidance. I would also like to thank my Special Committee Member, Dr. Brian Kirby, for the tremendous support and guidance he has offered me. I am extremely grateful for his time and invaluable advice. I wish to sincerely thank Dr. Harold Craighead for his excellent guidance and incredible patience.

Additionally, I would like to express my great appreciation to Dr. Margaret Frey for her research guidance and help with the nanofiber-related aspects of my work. I would also like to thank my laboratory colleagues, Lauren Matlock-Colangelo, Dr. Katie Edwards, Barbara Leonard, Alden Sonnenfeldt, and Aditi Naik, for all of their help.

I wish to thank my wonderful parents, Tim and Heather Reinholt, for their continual support and encouragement of my academic pursuits. I would also like to thank my sister, Rachel Reinholt, for always making me smile and laugh every time I visit. I wish to express my thanks to my brother, Brian Reinholt, for his love and support. I would also like to thank my boyfriend, Thomas Wild, for his unwavering love and support, and for always being there for me no matter what. I thank him for his understanding of the significant time I dedicated to my work that would have otherwise been happily spent with him.

Finally, I would like to acknowledge the support of the Cornell University, College of Engineering Lester B. Knight Fellowship. I am also grateful for the support provided by the National Science Foundation (NSF) under grant No. CBET-0852900. My work was performed in

part at the Cornell NanoScale Facility, a member of the National Nanotechnology Infrastructure Network, which is supported by the National Science Foundation (Grant ECCS-0335765). Also, my work was developed in part under the auspices of the Cornell University Center for Life Science Enterprise, a New York State Center for Advanced Technology supported by New York State and industrial partners. I also acknowledge partial support by a subcontract with Rheonix, Inc. and 1U01 A1082448-01 from the National Institutes of Health. Any opinions, findings and conclusions or recommendations expressed in this publication are mine and do not necessarily reflect the views of Rheonix Inc. nor those of the National Institutes of Health. Additionally, my work made use of the Cornell Center for Materials Research Shared Facilities which are supported through the NSF MRSEC program (DMR-1120296). I also appreciate the partial funding provided by the NC1194 Multistate Federal Hatch Project on Nanobiosensors.

TABLE OF CONTENTS

LIST OF FIGURES

LIST OF TABLES

LIST OF ABBREVIATIONS

ABTS	2,2'-Azinobis [3-ethylbenzothiazoline-6-sulfonic acid]-diammonium salt
AMV	Avian Myeloblastosis Virus
AO7	Acid Orange 7
AOM	Aluminum Oxide Membrane
BSA	Bovine Serum Albumin
cDNA	complimentary DNA
DNA	Deoxyribonucleic Acid
dNTP	Deoxynucleoside Triphosphates
EDC	1-Ethyl-3-(3-dimethylaminopropyl) Carbodiimide Hydrochloride
HDA	Helicase-Dependent Amplification
HEPES	N-(2-Hydroxyethyl)piperazine-N'-2-ethanesulfonic Acid
HRP	Horseradish Peroxidase
HSS	HEPES Sucrose Saline
ITP	Isotachophoresis
KB	polystyrene$_{8K}$-*block*-poly(ethylene-*ran*-butylene)$_{25K}$-*block*-polyisoprene$_{10K}$-Brij76
LAMP	Loop-Mediated Isothermal Amplification
LFA	Lateral Flow Assay
LOD	Limit Of Detection
MES	2-(N-Morpholino) Ethanesulfonic Acid
mRNA	messenger RNA
NA	Nucleic Acid
NASBA	Nucleic Acid Sequence-Based Amplification

NHS	N-Hydroxysuccinimide
PAMAM	Polyamidoamine
PBS	Phosphate-Buffered Saline
PCR	Polymerase Chain Reaction
PEG	Polyethylene Glycol
PLA	Poly(lactic acid)
PMMA	Poly(methyl methacrylate)
Poly-A	Poly-Adenosine
PVA	Poly(vinyl alcohol)
PVC	Polyvinyl chloride)
RCA	Rolling Circle Amplification
RNA	Ribonucleic Acid
RT	Reverse Transcription
rRNA	ribosomal RNA
SA:V	Surface Area-to-Volume Ration
SEM	Scanning Electron Microscopy
siRNA	small interfering RNA
SRB	Sulforhodamine B
SSC	Saline Sodium Citrate
TBO	Toluidine Blue O
Tris	2-Amino-2-hydroxymethyl-propane-1,3-diol
µPAD	Microfluidic Paper Analytical Devices
µTAS	Micro Total Analysis System

CHAPTER 1

MICROFLUIDIC NUCLEIC ACID ISOLATION

Abstract

Nucleic acid (NA) detection within micro total analysis systems (μTASs) for point-of-care use is a rapidly developing research area. For these systems to be maximally effective, efficient NA isolation from the raw sample is crucial, and using microfluidics assists in reducing sample sizes and reagent consumption, increases speed, avoids contamination, and enables automation. Through miniaturization into microchips, new techniques have been realized that would be unfavorable and inconvenient to use on the macro-scale, but provide an excellent platform for micro-scale NA purification. In this review, the complexities of NA isolation, as well as the considerations when choosing a technique for microfluidic NA isolation, are discussed, in addition to the numerous NA isolation techniques that have been miniaturized and integrated into microfluidic devices. Here, their advantages and disadvantages, as well as their (potential) applications, are included. The techniques presented include using silica-based surfaces, functionalized paramagnetic beads, oligonucleotide-modified polymer surfaces, pH-dependent charged surfaces, aluminum oxide membranes, and liquid-phase isolation.

1 Introduction

The development of bioassays for the detection of nucleic acids (NAs) has provided a monumental technological advancement in numerous fields of study with applications including pathogen detection in food, environmental, and clinical samples, as well as genetic analysis.[1-9] These assays provide several advantages over traditional microbiological methods that require the use of culturing techniques, such as reduced time and applicability to microorganisms and cells

that cannot be grown under laboratory conditions. A crucial part of NA detection assays is the isolation of the NAs. Without adequate purification of NAs from the raw samples, the sensitivity of the device is greatly decreased, and downstream processes, such as amplification and detection, could be inhibited.

The detection of nucleic acids has been well-established using bench top, macro scale techniques; however, these techniques often require large specialized equipment, trained personnel, large sample sizes, and are generally time-consuming and expensive, which normally limits them to usage in centralized laboratory facilities. Consequently, there has been a strong interest in the development of portable point-of-care devices that can be used in resource-limited settings. As a result, the concept of a micro total analysis system (μTAS), or lab-on-a-chip, was presented by Manz *et al.*[10,11] These miniaturized analytical devices provide a significant improvement in performance. The major potential advantages of miniaturizing NA detection assays are that they require a much smaller sample volume, consume smaller quantities of reagents, and are faster and more sensitive due to their small size. Additionally, because these assays are carried out completely within a single device, the risk of contamination is almost eliminated and the system can be automatable. In order to take full advantage of miniaturized lab-on-a-chip systems for NA detection, isolation of NAs must be effectively done inside a device. Furthermore, unique advantages can and should be exploited, rather than just attempting to copy macro scale techniques and shrink them down to the micro scale, so that lab-on-a-chip systems can reach their full capabilities. Here, the non-user interference, non-contamination, fast diffusion, short reaction distances, fast heat transfer, and simple extraction capabilities are of ultimate importance.

Isolation of NAs is a crucial step in a μTAS for the detection of cells and specific NA sequences in disease control, pharmacological studies, environmental protection, and fundamental

studies in which findings are tied to the identification of specific NA sequences. Critical sample aspects have to be considered prior to choosing the most appropriate NA isolation method in addition to the most obvious one, i.e. in the typically complex biological[12] and environmental[13] samples in which cells are contained. Cell lysis is the first step in NA isolation that can be accomplished using a variety of techniques both on- and off-chip, which have been reviewed extensively in literature.[12,14] The lysate contains several contaminants, including proteins, cellular membrane debris, polysaccharides, metabolites, ions, and other NAs,[15-17] that must be removed in the NA isolation process prior to subsequent analysis stages. The different types of NAs present in cells, including DNA, mRNA, rRNA, siRNA, etc., each have their own unique characteristics, such as function, mass, abundance, and location within the cells.[18]

Another set of critical decision points is the type of NA to be isolated, the purpose for its isolation, and the complexity of required operations as these need to be realized in a limited space within a µTAS chip. Figure 1 summarizes relevant aspects of these decision points, which guide the researcher and user in the definition of critical device and assay characteristics. This review delivers a comprehensive overview of NA isolation techniques carried out within microdevices. The main techniques discussed within are silica-based surfaces, functionalized paramagnetic beads, oligonucleotide-modified polymer surfaces, pH-dependent charged surfaces, aluminum oxide membranes, and liquid-phase isolation. The different methods are compared in terms of advantages and disadvantages as well as their performance in specific applications. Integration of microfluidic NA isolation into complete µTASs enables the development of rapid, sensitive, and portable NA detection assays that can be used in resource-limited settings. A brief summary of the reviewed articles and critical analysis of the advantages and disadvantages of the different nucleic acid techniques is given in Table 1.1.

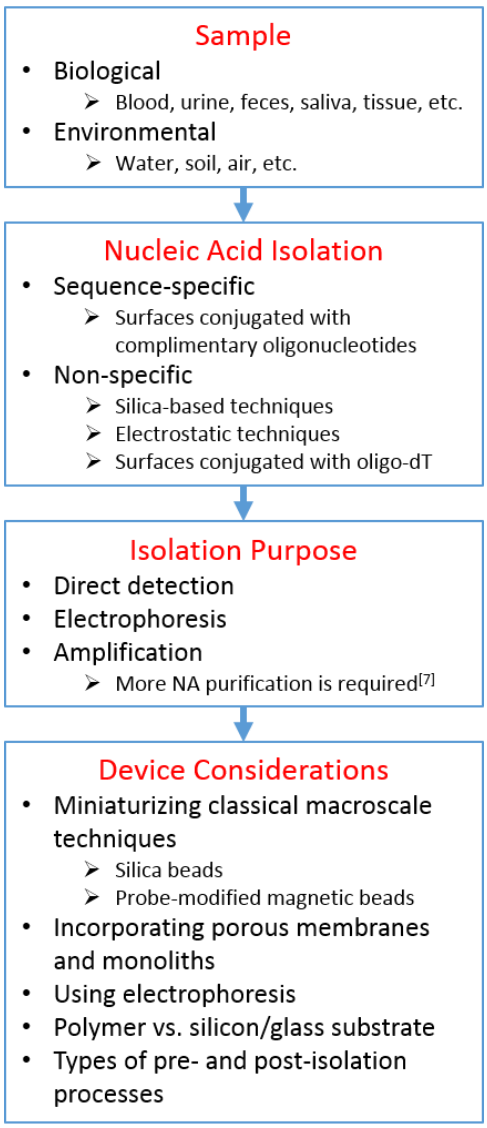

Figure 1.1: Critical decision points for choosing the appropriate NA isolation technique. Aspects that must be considered when deciding on a technique include the sample type, the specificity of the isolation, the isolation purpose, and the device characteristics and restrictions.

2 Microfluidic Nucleic Acid Isolation Techniques

2.1 Silica-Based Techniques

Silica-based techniques were developed and investigated early on in microfluidic devices mimicking the successful silica-based isolation techniques of the Boom technology from the 1990s

that is currently commercialized by bioMérieux.[20-22] Here, the non-specific binding of NA molecules to silica is being exploited for separation from other sample components. Chaotropic salts, such as guanidinium and sodium iodide, shield the negative charge of the silica surface, which decreases NA repulsion, and dehydrate the silica and NAs creating a hydrophobic environment, so that favorable hydrogen bonding occurs between the NAs and silanol groups.[23] With the NAs bound to silica, a wash with an organic solvent, such as ethanol or isopropanol, results in highly purified NAs upon elution into a low-ionic strength solution.

This chemical principle has been exploited in a variety of microfluidic designs combining the strengths of microfabrication and silica chemistry. Microscopic images of some of these platforms are depicted in Figure 1.2. Microfluidic devices initially copied the macro-principle of packed silica beads or the inclusion of silica beads in polymer matrices. Shortly thereafter, silica microstructures were proposed as the next step in streamlining device manufacturing and customization.

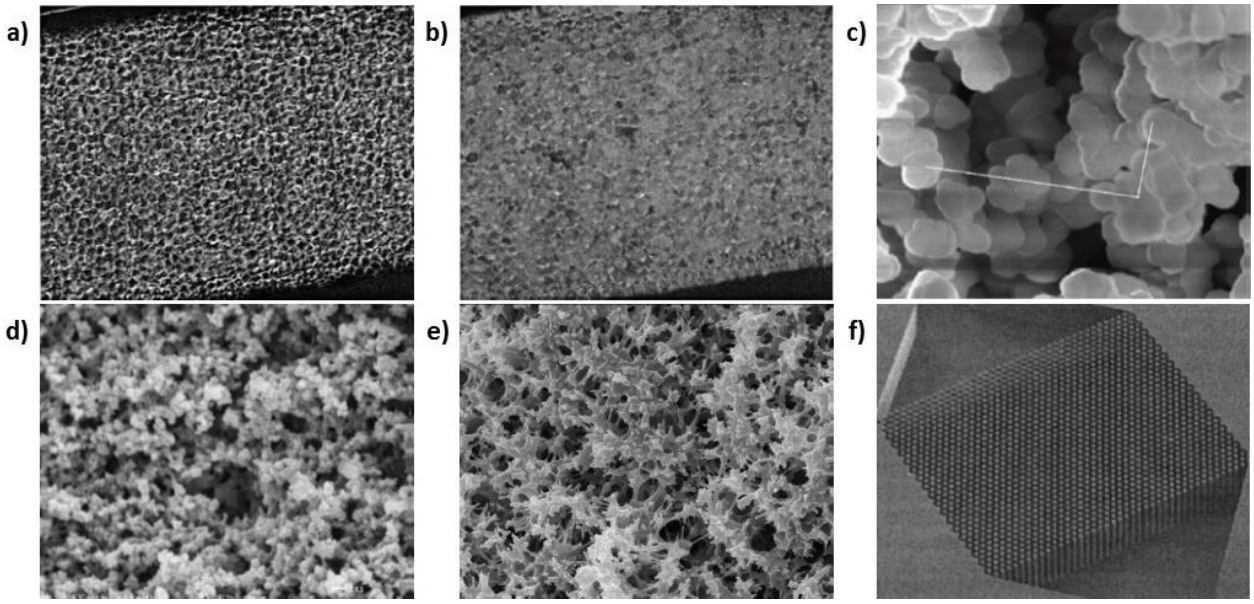

Figure 1.2: Microscopic images of the different silica-based surfaces used for NA isolation. **a)** silica beads within a microchannel *(reprinted with permission from K. A. Wolfe, M. C. Breadmore, J. P. Ferrance, M.*

*E. Power, J. F. Conroy, P. M. Norris, J. P. Landers, Electrophoresis **2002**, 23, 727–733. Copyright 2002 WILEY-VCH Verlag GmbH.),* **b)** silica beads incorporated into a sol-gel within a microchannel *(reprinted with permission from K. A. Wolfe, M. C. Breadmore, J. P. Ferrance, M. E. Power, J. F. Conroy, P. M. Norris, J. P. Landers, Electrophoresis **2002**, 23, 727–733. Copyright 2002 WILEY-VCH Verlag GmbH.),* **c)** silica beads incorporated into a porous polymer monolith *(reprinted with permission from A. Chatterjee, P. L. Mirer, E. Z. Santamaria, C. Klapperich, A. Sharon, A. F. Sauer-budge, Analytical chemistry **2010**, 82, 4344–4356. Copyright 2010 American Chemical Society.),* **d)** silica-based sol-gel *(reprinted with permission from Q. Wu, J. M. Bienvenue, B. J. Hassan, Y. C. Kwok, B. C. Giordano, P. M. Norris, J. P. Landers, J. P. Ferrance, Analytical chemistry **2006**, 78, 5704–10. Copyright 2006 American Chemical Society.),* **e)** silica-based porous polymer monolith *(reprinted with permission from K. J. Shaw, L. Thain, P. T. Docker, C. E. Dyer, J. Greenman, G. M. Greenway, S. J. Haswell, Analytica chimica acta **2009**, 652, 231–3. Copyright 2009 Elsevier.),* and **f)** silica micropillar array (reprinted with permission from L. A. Christel, K. Petersen, W. McMillan, M. A. Northrup, Journal of biomechanical *engineering **1999**, 121, 22–7. Copyright 1999 ASME.).*

2.1.1 Packed Silica Beads

Silica beads have been used in NA purification for over two decades, starting with benchtop assays using spin columns packed with silica beads.[20,29-31] This concept was miniaturized by incorporating silica beads into microcapillaries for more rapid NA isolation without the need for lengthy centrifugation.[32,33] For example, Tian *et al.* demonstrated the use of microcapillaries packed with only nanograms of silica beads to extract λ and prepurified human genomic DNA with approximately 70% efficiency, and reported a capacity of 10-30ng of DNA per mg of beads.[33] The majority of microfluidic devices constructed for the use of packed silica beads incorporate a weir structure, which acts as a frit to confine the beads to a specific location within the channel while still allowing fluid flow.[34] Zhong *et al.* developed a reusable device yielding an efficiency of 80% of λ DNA extracted [35]. Hagen *et al.* were the first to demonstrate successful on-chip isolation of RNA using packed silica beads.[36] Combining the NA isolation directly with an amplification reaction is the ultimate goal of a μTAS, and has been demonstrated for DNA isolation using packed silica beads and PCR amplification on-chip.[37,38] Here, it was important to thoroughly remove the solid phase extraction reagents, such as the chaotropic salts and organic solvents, as these are known PCR inhibitors.[38] These microfluidic devices contained separate

channels/reservoirs for DNA isolation and PCR amplification to further prevent inhibitors from interfering with PCR.[37,38] However, as Wolfe *et al.* also demonstrated, results were often not reproducible and the stability of the bead bed was poor resulting in destruction of the microchip after prolonged use,[24] which limits the usefulness of packed beads in μTAS applications. Additionally, issues such as bead compaction, increasing back pressure and decreasing flow due to the dynamic nature of bead packing are common drawbacks. A solution for several of these challenges has been found by entrapping the silica beads in polymer matrices within the microfluidic devices.[24]

2.1.2 Silica Bead-Containing Matrices

To improve upon the use of silica beads, they have been confined within porous materials, such as sol-gels and porous polymer monoliths. In the case of sol-gels, silica particles are incorporated into the gelation or polycondensation process[39] resulting in a monolith for NA isolation. Wolfe *et al.* investigated tetraethoxysilane (TEOS) sol-gels containing silica particles for DNA isolation.[24] The authors focused on the identification of the most relevant factors that resulted in effective DNA isolation, which were the size of the silica beads, the material used for the sol-gel, the type of condensation reaction, and the monolith construction method. Breadmore *et al.* followed-up by optimizing the extraction conditions using this ideal silica bead-incorporating sol-gel, and extracting DNA from whole blood, bacterial DNA, and viral DNA.[23] Here, loading conditions were examined and the pH and flow rate were optimized. A decreased pH resulted in decreased repulsion between the silica surface and the DNA molecules, which in turn resulted in an increased DNA adsorption rate. This also enabled higher flow rates, and DNA extraction from whole blood was accomplished in under 15 minutes with an average efficiency of 67% over 10 successive extractions. Subsequently, Legendre *et al.* were the first group to demonstrate

successful DNA isolation and PCR amplification within the same microdevice.[40] A significant limitation of using sol-gel matrices is the high heat required that in turn necessitates the use of glass as the microfluidic platform, which is a relatively expensive material to pattern.

The Klapperich group has demonstrated a novel strategy to create porous polymer monoliths containing silica beads in order to use an inexpensive plastic-based microfluidic platform that can be patterned easily using hot-embossing. The significant decrease in manufacturing cost also allows these devices to be disposable, which obviously eliminates the risk of contamination between uses, and cleaning procedures that could be inadequate, too harsh leading to surface damage, or introduce additional inhibitors. These monoliths contain micro- and nano-scale pores, which allow fluid flow with low back pressures as well as a large surface area for NA adsorption.[41] Polymers, such as the cyclic olefin polymer, can be chosen that facilitate subsequent in-device detection due to their excellent optical qualities.[42,43] Initial designs achieved an extraction efficiency of 70±3%,[42] and were then successfully applied to a variety of conditions, including DNA from gram-positive and gram-negative bacteria in whole blood,[44] RNA from influenza virus type A in human nasopharyngeal aspirate,[43] DNA from *Clostridium difficile* in stool samples,[45] and DNA from *Escherichia coli* in urine.[46] Some of these assays have even been incorporated into μTASs integrating on-chip NA amplification.[45,47] While these methods of immobilizing silica beads within porous materials solve many of the problems associated with packed silica beads, they require additional fabrication steps once the microfluidic device is already fabricated, and they are occasionally difficult to reliably reuse.

2.1.3 Silica Microstructures

Silica microstructures have been developed to create a NA binding surface during the

microdevice fabrication itself, so that no post-fabrication processes are required. Since significantly less back pressure is observed in these devices in comparison to packed beads[35,36] and matrices,[33,42-44] higher flow rates can be realized, which in turn increases the throughput and allows for the processing of larger volumes. These devices are generally fabricated from silicon or glass substrates using reactive ion etching (RIE) to pattern the micropillars.[28,48-50] Here, maximizing the available surface area and mixing within the device are key to optimizing their extraction efficiency. Thus, the efficacy of the isolation device is heavily dependent on the silica surface area, as well as microstructure and microchannel shapes.

The surface area of the isolation device is determined by the size and density of the microstructures as well as the overall size of the isolation chamber. Generally, the surface area-to-volume ratio (SA:V) is chosen as a compromise between maximizing surface area, ease of fabrication, and flow rate limitations due to back pressure, which ultimately dictates the extraction efficiency. It was found that the extraction efficiency scales positively with SA:V and negatively with flow rate. Thus, Cady *et al.* fabricated an array of square micropillars that were very densely distributed, which resulted in a very large SA:V of 4200cm^2/mL.[48] With flow rates under 10µL/min, a respectable extraction efficiency of 77% was obtained. In contrast, Christel *et al.* fabricated a device with a lower density of square micropillars resulting in a smaller SA:V, but were able to use a higher flow rate (30µL/min).[28] The lower extraction efficiency of 50% was compensated with an increased sample volume due to the higher feasible flow rate. The flow rate phenomenon was also demonstrated by West *et al.* within the same microdevice.[50] The extraction efficiency at 500µL/min was just 55% percent of that at 5µL/min.

As indicated above, shape of the microstructures and of the microfluidic channels are important for determining an ideal flow pattern. Comparing microstructures with frustoconical and

pyramidal shapes, Wu *et al.* found that a bed of pyramidal pillars had a higher extraction efficiency than the frustoconical pillars. [51] It is hypothesized that the pyramidal pillars provide an increased flow disturbance, and therefore increase the number of DNA molecules that contact the binding surface. In the case of the microfluidic channel dimensions, a wider, shorter channel will reduce the hydrodynamic resistance and allow for higher flow rate, while a thinner, longer channel increases it.[50] If the device will be used for small sample volumes that contain little target NA, then a thin, long channel would be better to maximize the number of NAs that bind. For large sample volumes that contain more target, a wide, short channel would be more ideal as it would allow for a higher flow rate, and thus increased throughput, while compromising on the extraction efficiency. Figure 1.3 contains a diagram summarizing the design considerations for fabricating silica microstructures within microfluidic channels for NA isolation.

The integration of silica microstructure technology into a μTAS, including NA amplification and detection steps, has been demonstrated. Wu *et al.* have extracted DNA from A549 cells and whole blood with subsequent on-chip loop-mediated isothermal amplification (LAMP) and fluorescence detection.[51] They were able to achieve extraction efficiencies that were equal to or better than a commercial kit. Cady *et al.* developed a microdevice that detects *Listeria monocytogenes* in 45 minutes with a limit of detection (LOD) of around 10^4 cells.[52] This device used an array of square micropillars for DNA isolation and real-time PCR to amplify and fluorescently detect the DNA.

In summary, silica microstructure arrays can be used as an effective NA isolation platform. The main disadvantages of this isolation technique are that the devices are constructed from relatively expensive materials and the manufacturing process is complex, time-consuming, and requires access to a cleanroom, which is very costly.

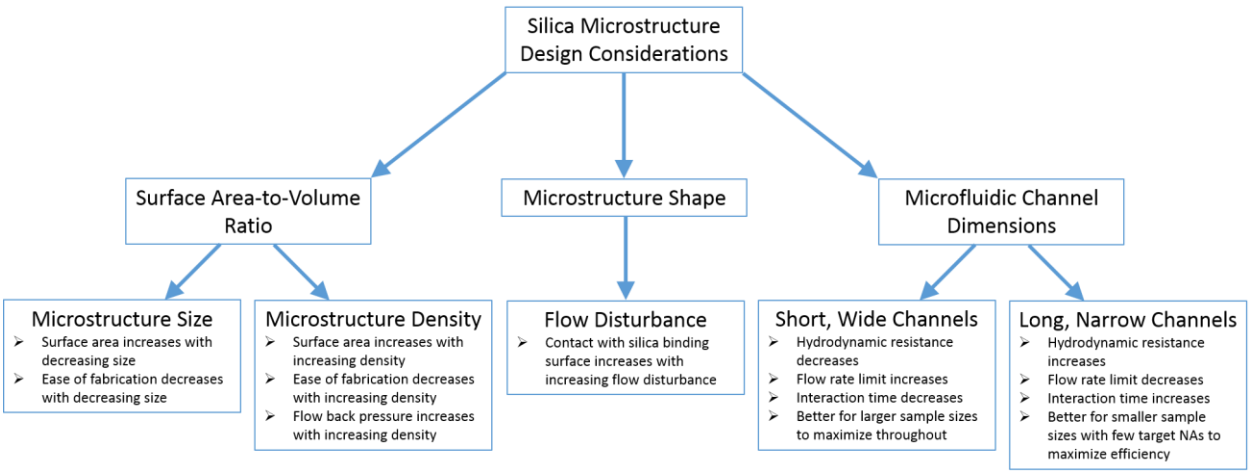

Figure 1.3: Summary of design considerations for the fabrication of silica microstructures for NA isolation. Critical characteristics of the microstructures include their size, density, and shape. Selection of the appropriate dimensions for the microfluidic channels is also very important and should be made based on the sample size and concentration.

2.1.4 Other Silica-Based Surfaces

Other silica-based surfaces for NA isolation have been used within microfluidic devices, including silicate-based porous polymer monoliths and silica membranes in order to avoid issues such as bead compaction, uneven distribution of beads within matrices, and the high cost of microfabrication. Several groups have used porous polymer monoliths made from tetramethyl orthosilicate (TMOS)[26,53] and potassium silicate solutions.[54-56] For example, Wu *et al.* were the first to use TMOS monoliths for DNA extraction, demonstrating an extraction efficiency of 85% with λ DNA in solution and 70% with human genomic DNA in whole blood.[26] Wen *et al.* developed a two-stage system in which proteins were removed from the sample using a C18 reversed-phase monolith, and subsequently DNA from whole blood with a TMOS monolith.[53] With their design, only 38% of the DNA was extracted without the protein removal stage, but with this stage, 69% of the DNA was retained. We propose that this type of pre-isolation protein removal could be applied to other technologies to achieve a higher extraction efficiency. Potassium silicate monoliths have been used to successfully extract DNA from buccal[54] and *Mus musculus*

cells,[56] as well as RNA from rat hepatocytes.[55] Kashkary *et al.* were able to isolate DNA from very small, dilute samples containing less than 15ng of DNA.[56] With small volumes of dilute sample, it is traditionally[57] suggested to use carrier RNA to reach sufficient extraction efficiencies.[27] However, Kashkary *et al.* were able to extract DNA from these sample without the use of a carrier, and achieved an extraction efficiency of approximately 85%.[56] Porous polymer monoliths without silica beads still possess a very large SA:V, and have been proven to sufficiently isolate NAs.

A yet different format for silica-based NA isolation is the use of silica membranes consisting of a network of glass fibers. Typically, the glass fiber membranes are integrated into the devices by simply physically securing them within a chamber. This approach has been used within complete μTASs to perform the NA purification step of the assays before amplification by PCR. The membranes have been used to isolate DNA and RNA from several different sample types, including bacterial DNA from *Bacillus cereus* and viral RNA from HIV I in saliva,[58] and G6PDH and BCR-ABL cancerous RNA transcripts from K562 cells in blood.[59] Using their device incorporating on-chip lysis, NA isolation, PCR (or RT-PCR), amplicon labeling, and detection, Chen *et al.* were able to achieve LODs of 10^3-10^4 *B. cereus* cells and 10^5 HIV virions/mL.[58] Kokoris *et al.* were able to detect cancer RNA transcripts from as few as 10 malignant cells.[59] In all cases, the NA isolation step within these devices was essential for achieving such low LODs. Schematics of each of the silica-based isolation techniques can be seen in Figure 1.4.

2.2 Paramagnetic Bead-Based Techniques

Separation assays using paramagnetic beads have been extensively used since the 1970s, and have been thoroughly reviewed in the literature.[60-63] Furthermore, paramagnetic beads have

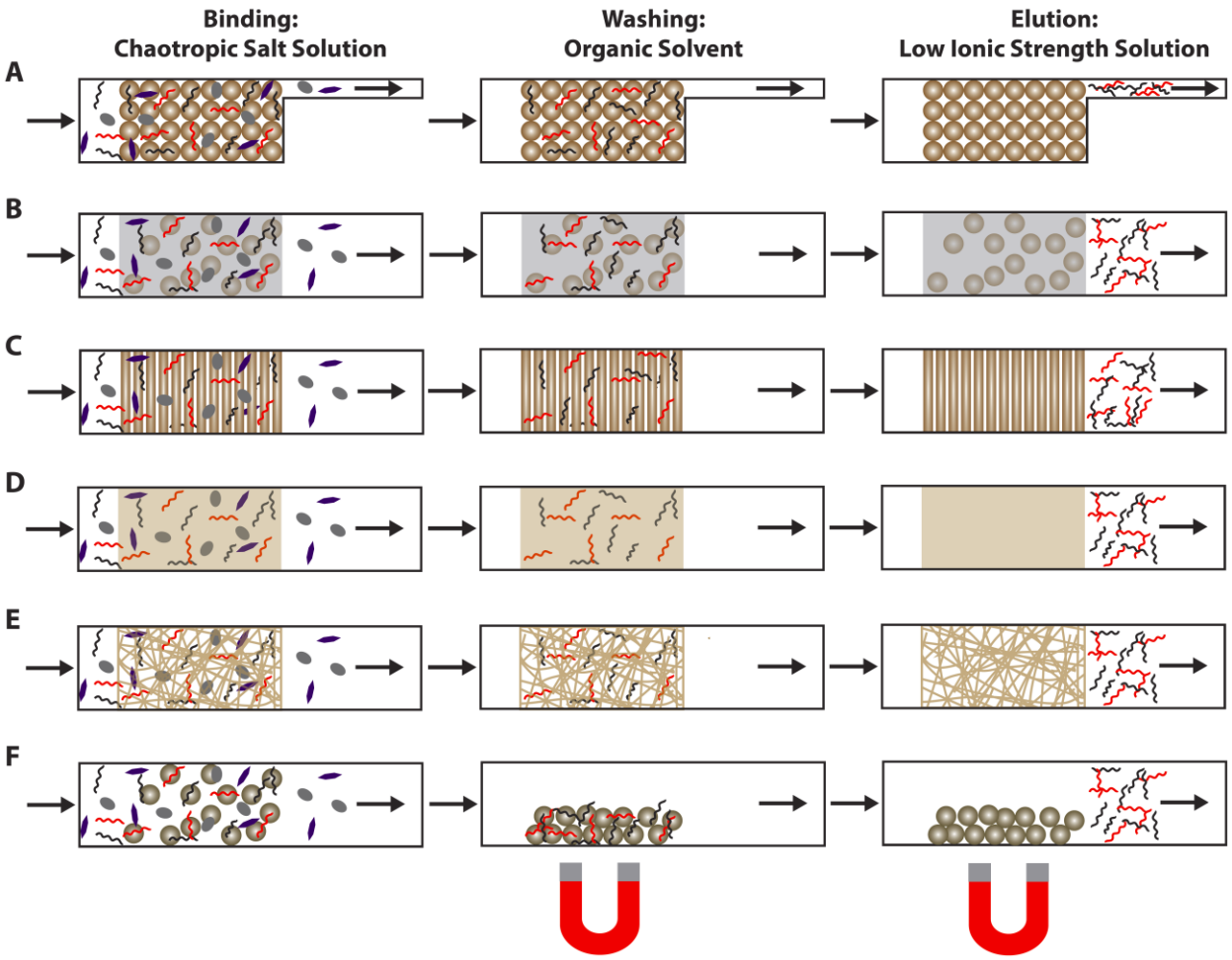

Figure 1.4: Schematic summary of silica-based NA isolation techniques. Silica-based isolation methods include: packed silica beads (A), silica beads embedded in matrices (B), silica microstructures (C), silica-based porous monoliths (D), silica membranes (E), and silica-coated paramagnetic beads (F).

been integrated into biological assays within microfluidic devices.[64,65] Paramagnetic beads have several advantages over packed bead beds in NA isolation assays. Crude samples with many solid contaminants of varying sizes are more easily dealt with as there is no issue of clogging due to densely-packed beads. A wide range of sample volumes can also be accommodated, since the beads still possess a large SA:V and the flow rate is not restricted by small pore sizes between packed beads and the weir structure. These advantages are possible due to the ability of the paramagnetic beads to be manipulated by a magnetic field. This allows the beads to be freely

suspended in the sample solution, which maximizes the interaction between the beads and sample, and it allows the beads to be collected using a magnetic field rather than centrifugation or filtration. Additional benefits are realized when using paramagnetic beads within a microfluidic device because much fewer beads can be used regardless of the sample volume, which reduces cost, and a lower magnetic field strength can be used, since the platform is a micro scale device. However, requiring a magnetic field puts limitations on the design of the microfluidic chip. The type of material and its thickness will affect the strength of the magnetic field,[64] and the microchannel should be designed to minimize bead loss. Both specific and non-specific NA isolation have been demonstrated through the use of paramagnetic beads with different surface modifications.

2.2.1 Silica-Coated Paramagnetic Beads

The general technique of using silica beads as described above can be enhanced by using silica-coated paramagnetic beads. Instead of being packed and confined to the chamber using a weir, paramagnetic silica beads can be free in solution and then be collected using a magnetic field, which increases the available silica surface area for NA binding. A schematic of this technique is shown in Figure 1.4. A variety of techniques have been employed for the washing and elution phases of NA isolation. There are conventional techniques that use a magnetic field to hold the beads stationary while washing buffers flow through the microchannels, and there are more unconventional techniques that use a magnetic field to move the paramagnetic beads through stationary washing solutions. Duarte *et al.* compared polyester-toner (PeT) devices versus glass devices using paramagnetic beads and a rotating magnetic field for agitation, and showed that the extraction efficiency was slightly higher for PeT (~70%) than glass (~64%) with elution occurring much more rapidly in PeT than in glass (73.5% vs. 34% in the first 6µL).[64] It was hypothesized that the thinner walls of the PeT device allowed a stronger magnetic field presence in the

microchannel, which increased the agitation of the beads resulting in faster elution. They also demonstrated scaling up to 8 PeT microchannels, but also showed that the nonhomogeneity of the magnetic field between channels results in a lower average extraction efficiency across all the channels. Lien *et al.* integrated silica paramagnetic bead isolation into a complete μTAS for detecting α-thalassemia-1 genetic deletions in saliva samples with an LOD of 12 pg/μL.[65]

Microfluidic devices using stationary solutions and flowing paramagnetic beads have been developed with varying geometries and complexities. Bordelon *et al.* used glass tubes with a series of solutions separated by air bubbles via surface tension and used a donut-shaped magnet to move paramagnetic beads successively through the solutions.[66] This resulted in an LOD for RSV-infected HEp-2 cells that was comparable to that of a commercially available kit, while providing a significant improvement in handling. Hydrophobic immiscible liquids have also been used to separate the aqueous washing and elution solutions,[67] as well as to serve as the washing phase between the binding and elution phases.[68] By using immiscible liquids instead of air, the carryover of the aqueous solutions between phases is very small.[68] On the downside of using silica-coated paramagnetic beads, they still require the use of chaotropic salts and organic solvents, which can interfere with downstream processes such as NA amplification.

2.2.2 Paramagnetic Beads with Switchable Charges

Similarly to silica surfaces, charged surfaces can also be used to isolate NAs from complex samples due to the charged nature of NAs. Some materials can possess different surface charges depending on the pH of the solution in contact with them. This phenomenon has been utilized for NA isolation using materials that switch between a positive charge for binding the negative NAs, and a negative charge for elution. This type of material has been coated onto paramagnetic beads

to take advantage of their additional benefits. Thus, Liu *et al.* used beads coated with a commercial material with switchable charges in a microfluidic device that performed both total RNA extraction from T98 cells and reverse transcription (RT).[69] With the lysate in a buffer with pH lower than 6.0, the paramagnetic beads are positively charged, which causes the NAs in the sample bind to them, and the contaminants can be washed away. With their microdevice, they were then able to isolate a slightly higher amount of RNA (47.2µg) compared to the manual procedure (32.5µg) using the same type of beads. These types of magnetic beads have also been incorporated into complete µTASs. Lien *et al.* demonstrated gDNA isolation from leukocytes in a device that included leukocyte purification, lysis, gDNA extraction, and PCR on-chip for the purpose of detecting single nucleotide polymorphism genotyping.[70] Furthermore, a multiplex µTAS that can handle 10 samples has been developed by Liu *et al.* that can detect *Mycobacterium tuberculosis* starting from saliva samples straight through to a visible fluorescent signal.[71] They were able to achieve an excellent LOD of just 10 bacteria, which demonstrates the great potential of using paramagnetic beads with switchable charges to develop highly sensitive µTASs. However, as a general disadvantage of these methods, it needs to be emphasized that this process still necessitates the use of DNases and RNases to degrade the unwanted types of NAs.

2.2.3 Paramagnetic Beads Coated with Oligo-dT

Non-specific isolation of all NAs sometimes requires additional purification steps to narrow down the sample to a specific target NA type. The large number of NAs in some samples can even saturate the silica surface thereby lowering the extraction efficiency of the target NAs. In eukaryotic organisms, most messenger RNA (mRNA) possess a poly-adenosine (poly-A) tail, and an elegant way to increase the specificity of NA isolation is the detection of mRNA using the thymidine oligonucleotide, oligo-dT. The oligo-dT will hybridize with the poly-A tail of all the

mRNA molecules, while other types of NAs do not bind. An additional bonus of mRNA detection is the fact that only viable organisms will have these present within the cell in contrast to general DNA sequence detection.[72] Specific mRNA extraction is also advantageous, since the quantity of mRNA is very small compared to total RNA yet multiple copies exist for each sequence. With oligo-dT-conjugated paramagnetic beads, Jiang and Harrison were able to isolate just 2.8ng of mRNA for the rare *Drosophila Melanogaster* bicoid gene in 0.85mg of total RNA (50% mRNA extraction efficiency) within a very simple Y-shaped device.[73] Marcus *et al.* reported isolations of picogram and subpicogram quantities of mRNA from single cells with an extraction efficiency of 80% using a more complex device that incorporated cell capture, cell lysis, mRNA purification, complimentary DNA (cDNA) synthesis, and cDNA purification.[74] Isolation with oligo-dT paramagnetic beads has also been scaled-up for high throughput as well as simplified for rapidity by Berry *et al.* in which they developed a device with standardized dimensions of microtiter plates for extracting 384 or 1536 samples in parallel.[75] In their device, the beads are magnetically pulled through an immiscible hydrophobic phase that separates the binding and elution solutions, and the mRNA bound to the beads is purified with hydrophilic contaminants remaining confined within the aqueous binding phase and the hydrophobic contaminants remaining confined within the immiscible hydrophobic phase. With this technique, mRNA from over 100 samples was isolated in just 10s. The principle of specific RNA isolation can be further specialized by moving toward the isolation of specific sequences as discussed next.

2.2.4 Paramagnetic Beads Coated with Specific Sequences

Modifying paramagnetic beads with specific oligonucleotide sequences is very advantageous as it facilitates the possibility of direct detection of target NA sequences without further purification, since the NA sequences of interest simply hybridize complimentarily to the

paramagnetic beads while the rest of the NAs and contaminants are washed away. An important parameter that needs to be considered when developing probe-conjugated paramagnetic bead-based isolation systems is the density of probes on the surfaces of the magnetic beads. If the probe density is too high, then isolation can be hindered by steric effects.[76,77] Conversely, if the probes are too sparse, non-specific binding to the bead surface can occur and contaminate the sample.[76] In an attempt to avoid steric hindrance when isolating circular *Escherichia coli* RNA, Yeung and Hsing introduced the sample into a solution of biotinylated specific oligonucleotide probes for binding, and then this solution was transferred to the streptavidinylated paramagnetic beads for capture.[76] This strategy was integrated into a complete μTAS, and an LOD of 10^2-10^3 bacteria was achieved. Several other μTASs have been developed using paramagnetic beads modified with specific sequences that are both rapid and sensitive. These include μTASs for detecting nervous necrosis virus RNA from water samples that achieved an LOD of 10-100fg,[78] methicillin-resistant *Staphylococcus aureus* DNA from sputum, serum, and milk samples with an LOD of 10fg/mL,[79] and influenza A and B viral RNA with LODs of 10^1-10^2 viruses.[80] The specific nature of the NA isolation in these systems enabled detection with very low LODs. However, the isolation of specific sequences may be hindered by the presence of large concentrations of bulk DNA and RNA present in a sample, and this requires specific attention, potentially with the development of a two-step procedure. As pointed out in Table 1.1, a general disadvantage of using magnetic beads is the sometimes prohibiting costs involved with high quality paramagnetic beads and at this point it limits their widespread use in developing areas. Figure 1.5 shows schematics of paramagnetic bead-based methods of NA isolation.

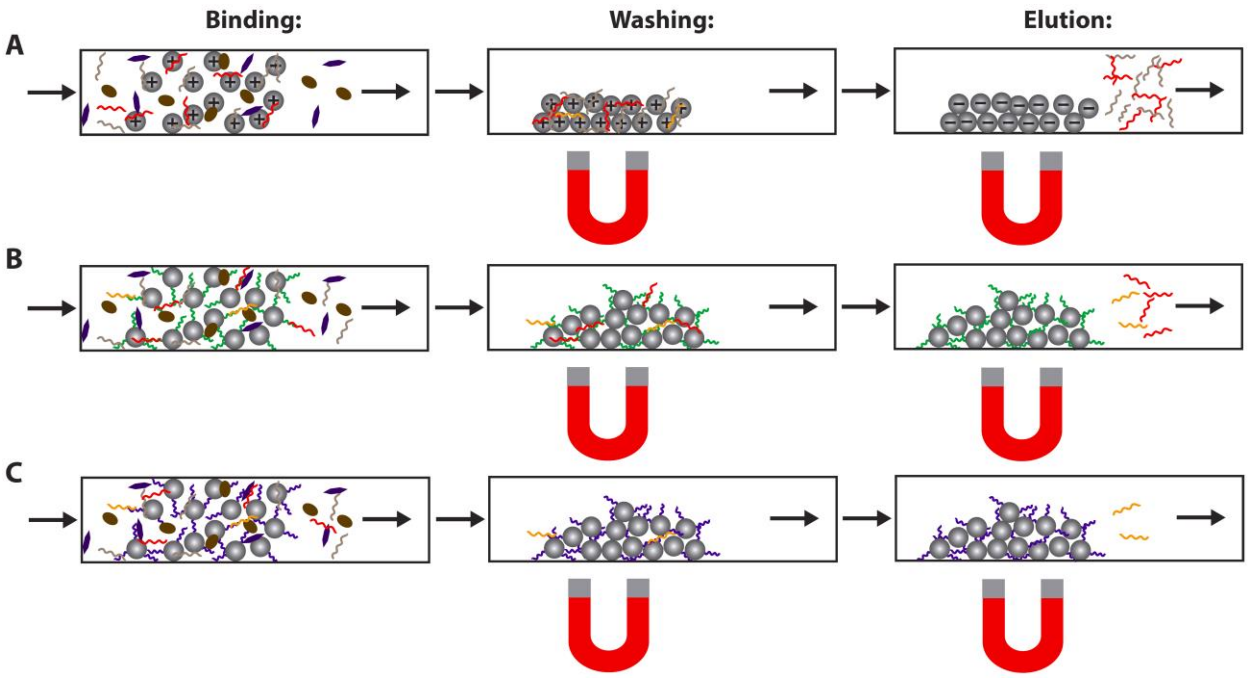

Figure 1.5: Schematic summary of paramagnetic bead-based NA isolation techniques. Isolation methods using paramagnetic beads include: paramagnetic beads with switchable charges (A), paramagnetic beads coated with oligo-dT probes (B), and paramagnetic beads coated with specific sequence oligonucleotide probes (C).

2.3 Specific Surface Modifications

Isolation of NAs can also be achieved by modifying a surface directly with oligonucleotides as well as using specific surfaces that will non-specifically bind NAs under certain buffer conditions. These methods are represented in the schematics in Figure 1.6 and are discussed below.

2.3.1 Oligonucleotides on Polymer Surfaces

Modifying polymer surfaces covalently with oligonucleotides for NA isolation is very advantageous as there is no need for beads, so restrictions on the dimensions of the device for confining the beads (packing or magnetic) are eliminated, as well as the cost of the beads. Synthesis

of these surfaces can be easily added to the manufacturing process; however, limiting the synthesis to isolated locations is only achievable using more complicated procedures, such as masks or alternate assembly designs.[81] Ultimately, microstructured fluidic channels similar to those presented above in the silica microstructured devices that are also modified with these surfaces should become most interesting, and cohesively create a platform for highly sensitive NA isolation.

Both oligo-dT and specific oligonucleotide probes have been immobilized onto porous polymer surfaces. Satterfield *et al.* demonstrated extraction of rat liver mRNA using oligo-dT_{30}-modified methacrylate polymer monoliths, and were able to extract greater than 16µg of mRNA in just 0.4µL of monolith with an extraction efficiency of 70%.[82] Root *et al.* used specific oligonucleotide probes to isolate the *gag* region of the HIV virus in serum samples, and achieved successful purification from concentrations as low as 37.5 copies/µL.[83] Creating these modified polymers within microfluidic channels requires additional steps that include reactive ingredients that could inhibit isolation or other processes if they are not adequately washed out; however, these polymers are needed to provide the additional surface area to immobilize a sufficient number of capture probes for effective NA isolation. Our group developed a method for modifying microchannels with a high immobilization efficiency without the need for synthesis of a porous matrix. Using 5^{th}-generation polyamidoamine dendrimers, oligo-dT probes were immobilized onto their periphery resulting in a high immobilization efficiency. Compared to probes immobilized in a monolayer on the surface of the microchannel, the use of dendrimers resulted in an 18-fold increase in the number of oligo-dT probes immobilized and a 16-fold increase in the amount of complimentary target captured.[72] Using probe modified surfaces as the isolation media would be very advantageous for µTAS applications in resource-limited locations as it simplifies the operation and reduces the cost of the device.

2.3.2 Chitosan-Coated Beads

The Landers group has developed an NA isolation technique using chitosan-coated beads. This is a non-specific isolation technique in which chitosan has a pH-dependent charge and can bind NAs at pH 5 and elute them at pH 9, which has great advantages over silica beads in that this procedure uses all aqueous buffers as opposed to chaotropic buffers and organic solvents that can inhibit downstream processes. Although chitosan surfaces have a lower overall capacity for NAs compared to silica surfaces, while still being sufficiently high for the desired applications, the elution of NAs is much faster with chitosan surfaces within a small elution volume. Hagen *et al.* found extraction efficiencies of 71% for chitosan beads versus 53% for silica beads.[84] Chitosan-coated beads have also been used within microfluidic devices to isolate RNA from buccal cells,[84] DNA from whole blood,[85] and RNA from the influenza A virus.[86] Advantages and disadvantages mentioned in general for bead-based microfluidic devices obviously also apply to these chitosan beads (see Table 1.1).

2.3.3 Aluminum Oxide Membranes

Aluminum oxide membranes (AOMs) can be used to isolate NAs in a similar way to silica membranes. A high salt concentration causes the NAs to bind to the membrane surface tightly. A positive characteristic of these membranes that has been exploited is that they will not inhibit PCR if the membrane volume relative to the PCR reaction volume is maintained below a certain threshold.[87] The NAs will in fact stay bound to the membrane in the presence of the PCR mix, so it can be used as a template in successive PCR reactions. Oblath *et al.* discovered that the NAs can be eluted when bovine serum albumin and *Taq* polymerase are added to the PCR reaction mixture.[88] AOMs have been incorporated into microdevices capable of isolating and amplifying

both RNA and DNA. Kim *et al.* successfully extracted and PCR-amplified DNA from just 300 *Bacillus cereus* cells and 2000 synthetic HIV RNA *gag* fragments.[87] A multiplex μTAS has also been developed that is capable of extracting, amplifying, and detecting just 300fg (100-125 copies) of genomic DNA from both methicillin-susceptible and methicillin-resistant *Staphylococcus aureus*.[88] The compatibility with downstream processing of samples makes AOMs very attractive NA isolation platforms. However, due to their tight binding of NAs, it is difficult to replenish the surface of the membrane, and replacement of the membrane with every sample presents its own challenges.

2.3.4 Photo-Activated Polycarbonate Surfaces

Photo-activated polycarbonate (PC) surfaces have been shown to non-specifically bind NAs in the presence of high concentrations of polyethylene glycol (PEG) and NaCl, based on the bench top demonstration of DNA binding to carboxylated magnetic beads by Hawkins *et al.*[89] Photo-activation of the PC creates a carboxylated surface, and the NA binding occurs in an analogous way to using silica surfaces. However, PC patterning is much easier and less expensive than silica surfaces, since it can be patterned using hot-embossing. Also, sodium polyanethole sulfonate (SPS), a commonly used anticoagulant for whole blood samples, is a known PCR inhibitor, and it binds to silica in the presence of chaotropic salts, but not to PC.[90] This technology was implemented into microfluidic devices, and first characterized in a sheet format by Xu *et al.*, achieving a loading density of 3.9 pmol/cm^2 for ssDNA sequencing ladders.[91] Based on these promising results, devices with micropost arrays within channels were fabricated and characterized by Witek *et al.*, and an extraction efficiency of 85% was attained for gDNA from whole cell lysates.[92] This technology has also been scaled up to a 96x format compatible with 96-well microtiter plates,[93] and has been used to purify gDNA and total RNA from whole cell lysates with

efficiencies of 63% and 73%, respectively.[90] These extractions were performed very quickly with 96 purifications taking less than 30 minutes, and the inexpensive nature of these devices enables them to be disposable. A limitation of using these surfaces could be the stability of the photo-activated surfaces over time and under various temperature conditions as is the case for applications in resource-limited settings.

2.3.5 Amine-Coated Surfaces

Amine-coated surfaces have been investigated for use in NA isolation within microfluidic chips. Amine groups are positively charged in buffers with a lower pH, and will non-specifically bind NAs through electrostatic interactions. These surfaces do not require buffers that contain species that can inhibit downstream processes, and amine surfaces can be generated in many ways on a variety of surfaces, which makes this technique simple and robust. Nakagawa *et al.* produced amine groups using amino silane compounds, and bound λ DNA and gDNA from whole blood using a buffer with pH 7.5 and eluted it using pH 10.6 buffer.[94] They were able to achieve efficiencies of up to 60%. These surfaces can successfully extract NAs; however, the solely electrostatic nature of the immobilization presents a surface that will attract any species with a negative charge. Also, the high pH of the elution buffer can also present problems for subsequent processes or necessitate pH adjustment.

2.4 Liquid-Phase Isolation Techniques

There have been other isolation techniques developed within microfluidic devices that do not use surfaces or probes as a means for binding NAs. These techniques utilize solution chemistry to separate NAs from the sample contaminants.

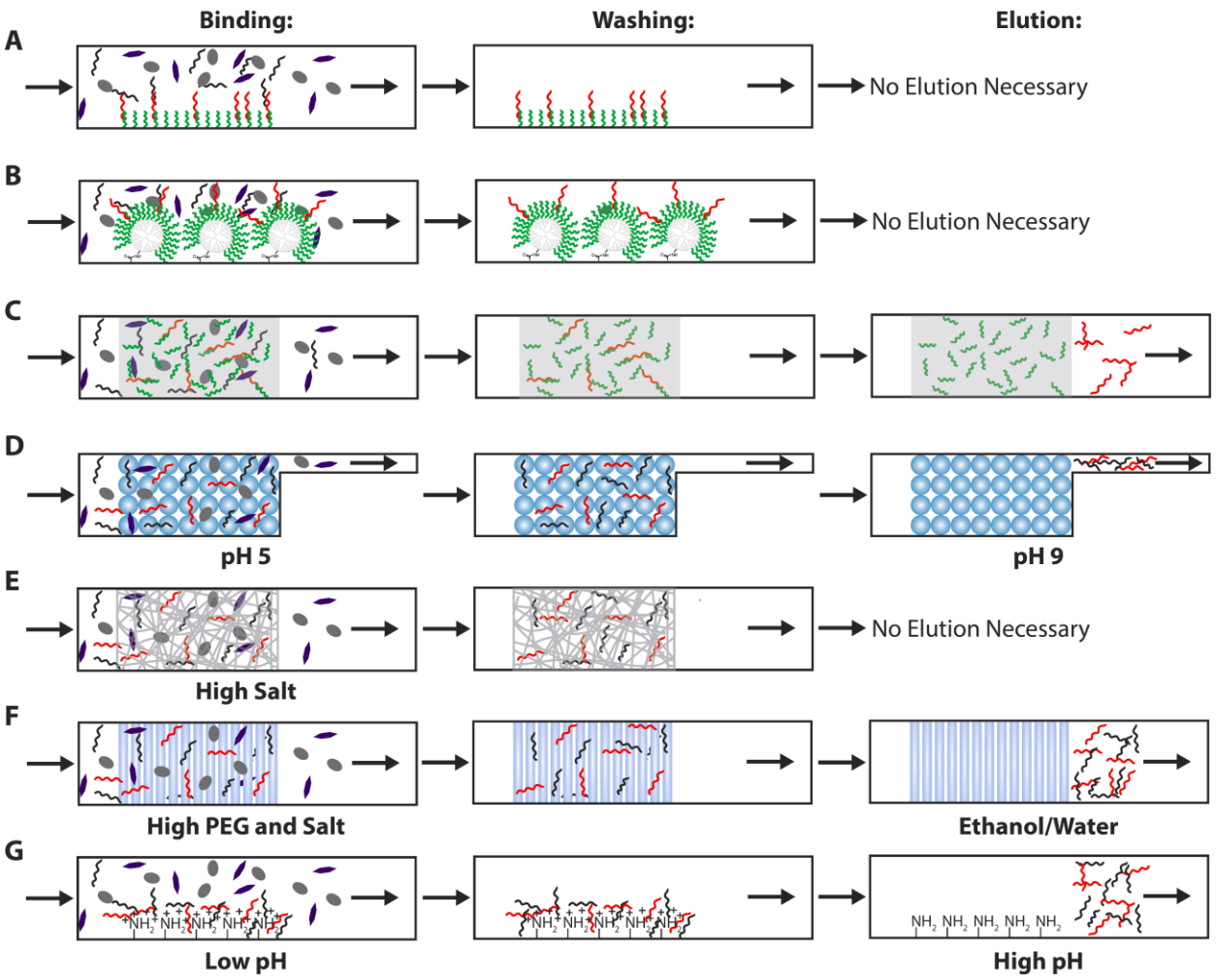

Figure 1.6: Schematic summary of NA isolation techniques using specific surface modifications. These techniques include: oligo-dT probes immobilized directly on the channel surface (A), oligo-dT probes immobilized on the periphery of dendrimers (B), oligonucleotide probes immobilized within a porous matrix (C), chitosan-coated packed beads (D), aluminum oxide membranes (E), photo-activated polycarbonate microstructures (F), and amine-coated surfaces (G).

2.4.1 Electrophoretic Techniques

Different techniques based on electrophoresis have been developed and integrated into microfluidic devices. For example, isotachophoresis (ITP) uses a two-buffer system containing a leading electrolyte and a trailing electrolyte that are designed to have electrophoretic mobilities higher and lower than the NAs, respectively. The trailing electrolyte should have a mobility lower

than the NA, but higher than the negative impurities. Positive impurities do not migrate in the same direction as the negative NAs. When an electric field is applied across the two buffers, the NAs migrate to the interface between the two buffers where an electric field gradient exists. This technology was demonstrated in a microchip by Persat *et al.*, with λ DNA achieving 100% extraction efficiency and extractions from whole blood achieving 30-70% efficiency.[95] Marshall *et al.* detected *Plasmodium falciparvum* DNA in whole blood with an LOD of 500 parasites.[96]

Another example is dielectrophoretic trapping. With this method, DNA can be trapped in areas of extremely large electric field gradients due to its polar nature. This is the same technology used by Nanogen Inc. to trap cells within their microdevices.[97] Prinz *et al.* successfully trapped chromatin from lysed *Escherichia coli* cells and separated it from other sample contaminants.[98] Here, an alternating current (AC) field was used to trap the chromatin, and a small direct current (DC) field was used to remove contaminants, including proteins, RNA, and cellular debris. The microdevice was designed with a specific geometry that controlled the location of the areas of high electric field gradient, and thus trapping areas.

Gel-electrophoresis has also been demonstrated within a microfluidic device for extraction of RNA from complex samples. Here, a DC constant current is applied to the microchannel containing the sample and negatively charged species migrate across with smaller, more charged species moving more quickly than the larger, less charged species. Using this technique, low molecular weight RNA was isolated from *Escherichia coli* and *Streptococcus thermophiles* bacteria lysate samples.[99] This was possible due to the small, highly negative nature of these RNAs and the gel, which acted as a cut-off filter for higher molecular weight species such as protein, cellular debris, and genomic DNA. This is another example of an established macro-scale process being scaled down into a microfluidic device.

These electrophoretic-based techniques for NA isolation have several advantages over typical solid-phase extraction. Firstly, there is no need for external pumps for pressure-driven flow; only a voltage source, so the overall size of the device is decreased. Secondly, the use of chaotropic salts and organic solvents that inhibit downstream processes is not necessary. Thirdly, these techniques are generally insensitive to the type substrate material used. Also, for ITP, the geometry of the microchannels does not affect the process. These advantages make these techniques attractive for the isolation of NAs, but there are some concerns as well. Most importantly, none of these technologies have been integrated into a microchip that also performs on-chip amplification or detection; they all require removal of the sample via pipette. Also, the electrophoretic mobility of the NAs to be isolated must be known, which varies with charge and dynamic size of the NAs.[100]

2.4.2 Organic Liquid Isolation

The well-established macro-scale technique of liquid-phase phenol-chloroform extraction has also been miniaturized and performed within a microfluidic device. In this process, proteins and cellular debris partition from the aqueous sample phase into the organic phase as it is an energetically-favorable transition. The main advantage of this technique over solid-phase extraction is that the purification efficiency is higher, which enables the successful extraction of minute quantities of NAs. In fact, using this technique on-chip, Zhang *et al.* were able to isolate DNA and RNA from 5000 bacterial cells down to just one cell in 1µL or 125nL of sample.[101] Furthermore, the resulting purified NAs were amplified via PCR in the same chambers where isolation occurred. This indicates the successful removal of inhibitors and isolation of target NAs. Sensitivity was likely improved by performing isolation and amplification within the same chamber, since NA losses during sample transfer are avoided, as also demonstrated previously in

our research.[72] From this range of bacterial sample sizes, the extraction efficiencies were an impressive 85-120%. The main disadvantage of this technique is the use of extremely hazardous organic solvents, which requires safe handling and disposal. This would clearly limit the use of these devices in most in-field, on-site, and resource-limited applications.

3 Conclusions

Summarized in Table 1.1, the NA isolation techniques discussed in this review demonstrate the potential to develop μTAS devices capable of being used in point-of-care settings. By miniaturizing these processes and integrating them into a microfluidic device, many advantages are realized compared to their macro scale bench top counterparts. Miniaturization also gives researchers numerous options for isolating NAs, as many different techniques have been demonstrated. This means the isolation method can be selected based on which technique is most suitable for the assay parameters, including sample type and size, device material and fabrication technologies available, as well as the pre- and post-isolation processes, instead of requiring the device and assay to be designed around the isolation technique. Scaling down NA purification into a microfluidic device can make the process more cost effective, faster, automatable, and reduce contamination. In addition, it enables these technologies to be multiplexed to handle multiple samples simultaneously, and provides a platform for high-throughput sample processing.

Although the development of NA isolation techniques within microdevices has advanced significantly with many different techniques being discovered, there is still great room for improvement both with the techniques themselves and integration and compatibility with other processes, such as cell lysis, NA amplification, and detection. Also, the ability to achieve close to

Table 1.1: Summary of Nucleic Acid Isolation Techniques

Isolation Technique	Advantages	Disadvantages	Isolation Application	Ref.
Packed Silica Beads	• Well established • Simple concept	• Bead compaction leading to increased back pressure and decreased flow • Not reliably reusable • Uses solutions that inhibit amplification • Device restrictions	RNA from neat semen, mock semen stain, and alveolar rhabdomyosarcoma	[36]
			B. anthracis DNA in whole blood and *B. pertussis* DNA in nasal aspirate	[37]
			Short tedem repeat (STR) DNA fragments in whole blood and semen	[38]
Sol-gels incorporating silica beads	• Large SA:V • Generally reusable	• Requires post-fabrication processing • High fabrication temperature • Expensive substrate • Uneven bead distribution • Uses solutions that inhibit amplification	*S. typhimurium* and *B. anthracis* DNA in whole blood	[23]
			Genomic DNA in whole blood and *B. anthracis* DNA in a nasal swab	[40]
Porous polymer monoliths incorporating silica beads	• Large SA:V • Disposable (one-time use) • Inexpensive	• Requires post-fabrication processing • Uneven bead distribution • Uses solutions that inhibit amplification	Influenza A viral RNA in cultured mammalian (MDCK) cells	[43]
			Influenza A and B viral RNA in a nasopharyngeal swab and aspirate	[47]
			E. coli DNA in urine	[46]
			E. coli, *B. subtilis*, and *E. faecalis* DNA in whole blood	[44]
			C. difficile DNA in stool	[45]
Fabricated Silica Microstructures	• No post-fabrication processing • Reusable • Higher flow rates feasible	• Expensive substrate • Long, complex, expensive fabrication process • Lower SA:V • Uses solutions that inhibit amplification	Genomic DNA from leukocytes in whole blood	[49]
			DNA from salmon sperm cells	[50]
			Genomic DNA in whole blood and A549 cell suspensions	[51]
			Bacterial DNA from *L. monocytogenes*	[52]
Silicate-based Porous Monolith	• Large SA:V	• Requires post-fabrication processing	Genomic DNA in whole blood	[26, 53]
			Genomic DNA from buccal cells	[54]
			RNA from rat hepatocytes	[55]

Table 1.1 (Continued)

		• Uses solutions that inhibit amplification	DNA from *Mus musculus* cells	[56]
Silica Membrane	• Easy integration into microfluidic device	• Expensive • Uses solutions that inhibit amplification	*B. cereus* DNA and HIV I viral RNA in saliva	[58]
			G6PDH and BCR-ABL cancer transcripts in K562 cells	[59]
Silica-coated Paramagnetic Beads	• High flow rates possible • Large SA:V	• Requires magnetic field • Device material and dimensions restrictions • Uses solutions that inhibit amplification • Beads are expensive	Genomic DNA in whole blood	[64]
			α-thalassemia-1 DNA genetic deletions in saliva	[65]
			RNA from RSV-infected HEp-2 cells	[66]
			RNA from HIV-1 virus in plasma	[68]
Paramagnetic Beads with Switchable Charges	• High flow rates possible • Large SA:V • Uses pH instead of PCR-inhibiting solutions	• Requires magnetic field • Device material and dimensions restrictions • Beads are expensive	RNA from T98 cells	[69]
			Single nucleotide polymorphism genotyping of genomic DNA from leukocytes	[70]
			DNA from *M. tuberculosis* in saliva	[71]
Paramagnetic Beads Coated with Oligo-dT	• Only captures mRNA • Detects viable organisms • High flow rates possible • Large SA:V	• mRNA poly-A tail is necessary • Probe density restrictions • Requires magnetic field • Device material and dimensions restrictions • Beads are expensive	Bicoid gene mRNA from *Drosophila Melanogaster*	[73]
			mRNA from a single NIH/3T3 cell	[74]
			Multiplex mRNA isolation from MCF-7 cells	[75]
Paramagnetic Beads Coated with Specific Sequences	• Direct capture of target • Lower LODs	• Probe density restrictions • Requires magnetic field • Device material and dimensions restrictions • Beads are expensive	Circular RNA from *E. coli*	[76]
			RNA from nervous necrosis virus in water samples	[78]
			DNA from methicillin-resistant *S. aureus* in sputum, serum, and milk	[79]
			RNA from influenza A and B viruses	[80]
	• No device restrictions		mRNA from *C. parvum*	[72]

Table 1.1 (Continued)

Oligonucleotides on Polymer Surfaces	• Large SA:V	• Requires post-fabrication processing • Uses reactive substances that can inhibit downstream processes	mRNA from rat liver cells	[82]
			Gag region RNA from HIV viruses in serum	[83]
Chitosan-coated Beads	• Uses pH instead of PCR-inhibiting solutions • Fast elution in small volume	• Lower capacity • Bead compaction leading to increased back pressure and decreased flow • Device restrictions	RNA from alveolar rhabdomyosarcoma cancer cells and buccal cells	[84]
			Genomic DNA from whole blood	[85]
			RNA from influenza A virus in a mock nasal swab	[86]
Aluminum Oxide Membranes	• Does not inhibit PCR	• Not reusable	DNA from *B. cereus* cells and synthetic HIV RNA *gag* fragments	[87]
			DNA from methicillin-susceptible and methicillin-resistant *S. aureus* in saliva	[88]
Photo-Activated Polycarbonate Surfaces	• Less expensive • Patterned easily • Does not bind SPS • Disposable	• Stability of activated surface over time and range of conditions	Genomic DNA from whole blood and RNA from *E. coli*	[90, 92]
			Multiplex DNA isolation from *B. subtilis*, *S. aureus*, and *E. coli*	[93]
Amine-coated Surfaces	• Uses pH instead of PCR-inhibiting solutions • Many ways to generate amine surfaces	• Attracts other negative species • High pH of elution buffer could inhibit downstream processes	Genomic DNA from whole blood	[94]
Electrophoretic Techniques	• No need for external pumps (smaller experimental setup) • Does not use PCR-inhibiting solutions • Insensitive to device material and dimensions	• Difficult to integrate downstream processes • Electrophoretic mobility of NAs must be known	Genomic DNA from whole blood via ITP	[95]
			DNA from *P. falciparvum* in whole blood via ITP	[96]
			Chromatin from *E. coli* via DEP trapping	[98]
			RNA from *E. coli* and *S. thermophiles* via gel-EP	[99]
Organic Liquid Isolation	• Well-established on macroscale • High purification efficiency • Accommodates very small samples	• Uses extremely hazardous organic solvents	Multiplex DNA and RNA isolation from *P. aeruginosa* and *S. aureus*	[101]

100% extraction efficiency with complex samples has yet to be realized. Wen *et al.* demonstrated using a protein removal step before NA isolation, which substantially increased the NA extraction efficiency.[53] These types of pre-isolation preparation steps can be implemented to improve the effectiveness of the device and move toward 100% efficiency. In the technologies reviewed here, very few of them were integrated into complete μTAS devices able to handle raw samples and take them through to detection. This will be a necessary step toward developing truly point-of-care devices that can be used in a variety of places, including resource-limited locations.

4 Scope of the Thesis

The work presented in this thesis is based upon the development of new techniques and materials that can be implemented into novel biosensors for the purpose of point-of-care applications. Firstly, a unique, very simple microfluidic device developed for isolation and NASBA-based amplification of mRNA from *C. parvum* lysate will be presented. This technology was developed to simplify the combination of these two techniques and improve upon the existing technology in terms of ease-of-use and sensitivity. Secondly, the integration of electrospun nanofibers into paper-based lateral flow assays will be discussed. Here, an enzymatic sandwich immunoassay was ultimately proven to be successful using functionalized nanofibers, and non-specific binding was also eliminated using nanofibers incorporating anti-fouling polymeric materials. Finally, a summary of the conclusions from the research presented as well as future outlooks and next steps will be discussed.

5 References

[1] J. R. Epstein, I. Biran, D. R. Walt, *Anal. Chim. Acta* **2002**, *469*, 3–36.

[2] L. J. Kricka, *Clin. Chem.* **1999**, *45*, 453–8.

[3] I. Palchetti, M. Mascini, *Analyst* **2008**, *133*, 846–54.

[4] J. Wang, *Anal. Chim. Acta* **2003**, *500*, 247–257.

[5] T. G. Drummond, M. G. Hill, J. K. Barton, *Nat. Biotechnol.* **2003**, *21*, 1192–9.

[6] E. Palecek, *Talanta* **2002**, *56*, 809–19.

[7] J. Wang, G. Rivas, X. Cai, E. Palecek, P. Nielsen, H. Shiraishi, N. Dontha, D. Luo, C. Parrado, M. Chicharro, et al., *Anal. Chim. Acta* **1997**, *347*, 1–8.

[8] N. L. Rosi, C. A. Mirkin, *Chem. Rev.* **2005**, *105*, 1547–62.

[9] R. G. Cotton, *Biochem. J.* **1989**, *263*, 1–10.

[10] A. Manz, N. Graber, H. M. Widmer, *Sens. Actuators, B* **1990**, *1*, 244–248.

[11] D. R. Reyes, D. Iossifidis, P.-A. Auroux, A. Manz, *Anal. Chem.* **2002**, *74*, 2623–36.

[12] J. Kim, M. Johnson, P. Hill, B. K. Gale, *Integr. Biol.* **2009**, *1*, 574–86.

[13] J. T. Keer, L. Birch, *J. Microbiol. Methods* **2003**, *53*, 175–183.

[14] R. B. Brown, J. Audet, *J. R. Soc., Interface* **2008**, *5*, S131–8.

[15] M. G. Murray, W. F. Thompson, *Nucleic Acids Res.* **1980**, *8*, 4321–4326.

[16] K. Wilson, *Current Protocols in Molecular Biology* **2001**, *00*, 2.4.1–2.4.5.

[17] J. Wen, C. Guillo, J. P. Ferrance, J. P. Landers, *Anal. Chem.* **2007**, *79*, 6135–42.

[18] P. J. Asiello, A. J. Baeumner, *Lab Chip* **2011**, *11*, 1420–30.

[19] I. G. Wilson, *Applied and environmental microbiology* **1997**, *63*, 3741–51.

[20] R. Boom, C. J. Sol, M. M. Salimans, C. L. Jansen, P. M. Wertheim-van Dillen, J. van der Noordaa, *J. Clin. Microbiol.* **1990**, *28*, 495–503.

[21] S. A. Rutjes, R. Italiaander, H. H. J. L. van den Berg, W. J. Lodder, A. M. de Roda Husman, *Appl. Environ. Microbiol.* **2005**, *71*, 3734–3740.

[22] K. Loens, K. Bergs, D. Ursi, H. Goossens, M. Ieven, *J. Clin. Microbiol.* **2007**, *45*, 421–5.

[23] M. C. Breadmore, K. A. Wolfe, I. G. Arcibal, W. K. Leung, D. Dickson, B. C. Giordano, M. E. Power, J. P. Ferrance, S. H. Feldman, P. M. Norris, et al., *Anal. Chem.* **2003**, *75*, 1880–6.

[24] K. A. Wolfe, M. C. Breadmore, J. P. Ferrance, M. E. Power, J. F. Conroy, P. M. Norris, J. P. Landers, *Electrophoresis* **2002**, *23*, 727–733.

[25] A. Chatterjee, P. L. Mirer, E. Z. Santamaria, C. Klapperich, A. Sharon, A. F. Sauer-budge, *Anal. Chem.* **2010**, *82*, 4344–4356.

[26] Q. Wu, J. M. Bienvenue, B. J. Hassan, Y. C. Kwok, B. C. Giordano, P. M. Norris, J. P. Landers, J. P. Ferrance, *Anal. Chem.* **2006**, *78*, 5704–10.

[27] K. J. Shaw, L. Thain, P. T. Docker, C. E. Dyer, J. Greenman, G. M. Greenway, S. J. Haswell, *Anal. Chim. Acta* **2009**, *652*, 231–3.

[28] L. A. Christel, K. Petersen, W. McMillan, M. A. Northrup, *J. Biomech. Eng.* **1999**, *121*, 22–7.

[29] D. N. Miller, J. E. Bryant, E. L. Madsen, W. C. Ghiorse, *Appl. Environ. Microbiol.* **1999**, *65*, 4715–24.

[30] R. A. Haugland, N. Brinkman, S. J. Vesper, *J. Microbiol. Methods* **2002**, *50*, 319–23.

[31] C. Kneuer, M. Sameti, E. G. Haltner, T. Schiestel, H. Schirra, H. Schmidt, C. M. Lehr, *Int. J. Pharm.* **2000**, *196*, 257–61.

[32] S. G. Bavykin, J. P. Akowski, M. Vladimir, V. E. Barsky, A. N. Perov, D. Mirzabekov, V. M. Zakhariev, A. D. Mirzabekov, *Appl. Environ. Microbiol.* **2001**, *67*, 922–928.

[33] H. Tian, A. F. Hühmer, J. P. Landers, *Anal. Biochem.* **2000**, *283*, 175–91.

[34] D. Erickson, D. Li, *Anal. Chim. Acta* **2004**, *507*, 11–26.

[35] R. Zhong, D. Liu, L. Yu, N. Ye, Z. Dai, J. Qin, B. Lin, *Electrophoresis* **2007**, *28*, 2920–6.

[36] K. A. Hagan, J. M. Bienvenue, C. A. Moskaluk, J. P. Landers, *Anal. Chem.* **2008**, *80*, 8453–60.

[37] C. J. Easley, J. M. Karlinsey, J. M. Bienvenue, L. A. Legendre, M. G. Roper, S. H. Feldman, M. A. Hughes, E. L. Hewlett, T. J. Merkel, J. P. Ferrance, et al., *Proc. Natl. Acad. Sci. U. S. A.* **2006**, *103*, 19272–7.

[38] J. M. Bienvenue, L. A. Legendre, J. P. Ferrance, J. P. Landers, *Forensic Sci. Int.: Genet.* **2010**, *4*, 178–86.

[39] L. L. Hench, J. K. West, *Chem. Rev.* **1990**, *90*, 33–72.

[40] L. A. Legendre, J. M. Bienvenue, M. G. Roper, J. P. Ferrance, J. P. Landers, *Anal. Chem.* **2006**, *78*, 1444–51.

[41] K. J. Shaw, E. M. Hughes, C. E. Dyer, J. Greenman, S. J. Haswell, *Lab. Invest.* **2013**, *93*, 961–6.

[42] A. Bhattacharyya, C. M. Klapperich, *Anal. Chem.* **2006**, *78*, 788–92.

[43] A. Bhattacharyya, C. M. Klapperich, *Sens. Actuators, B* **2008**, *129*, 693–698.

[44] M. Mahalanabis, H. Al-Muayad, M. D. Kulinski, D. Altman, C. M. Klapperich, *Lab Chip* **2009**, *9*, 2811–7.

[45] S. Huang, J. Do, M. Mahalanabis, A. Fan, L. Zhao, L. Jepeal, S. K. Singh, C. M. Klapperich, *PloS One* **2013**, *8*, e60059.

[46] M. D. Kulinski, M. Mahalanabis, S. Gillers, J. Y. Zhang, S. Singh, C. M. Klapperich, *Biomed. Microdevices* **2009**, *11*, 671–8.

[47] Q. Cao, M. Mahalanabis, J. Chang, B. Carey, C. Hsieh, A. Stanley, C. A. Odell, P. Mitchell, J. Feldman, N. R. Pollock, et al., *PloS One* **2012**, *7*, e33176.

[48] N. C. Cady, S. Stelick, C. A. Batt, *Biosens. Bioelectron.* **2003**, *19*, 59–66.

[49] H. M. Ji, V. Samper, Y. Chen, W. C. Hui, H. J. Lye, F. B. Mustafa, A. C. Lee, L. Cong, C. K. Heng, T. M. Lim, *Sens. Actuators, A* **2007**, *139*, 139–144.

[50] J. West, M. Boerlin, A. D. Jadhav, E. Clancy, *Sens. Actuators, B* **2007**, *126*, 664–671.

[51] Q. Wu, W. Jin, C. Zhou, S. Han, W. Yang, Q. Zhu, Q. Jin, Y. Mu, *Anal. Chem.* **2011**, *83*, 3336–42.

[52] N. C. Cady, S. Stelick, M. V. Kunnavakkam, C. A. Batt, *Sens. Actuators, B* **2005**, *107*, 332–341.

[53] J. Wen, C. Guillo, J. P. Ferrance, J. P. Landers, *Anal. Chem.* **2007**, *79*, 6135–42.

[54] K. J. Shaw, D. A. Joyce, P. T. Docker, C. E. Dyer, G. M. Greenway, J. Greenman, S. J. Haswell, *Lab Chip* **2011**, *11*, 443–8.

[55] K. J. Shaw, E. M. Hughes, C. E. Dyer, J. Greenman, S. J. Haswell, *Lab. Invest.* **2013**, *93*, 961–6.

[56] L. Kashkary, C. Kemp, K. J. Shaw, G. M. Greenway, S. J. Haswell, *Anal. Chim. Acta* **2012**, *750*, 127–31.

[57] R. H. Schiestl, R. D. Gietz, *Curr. Genet.* **1989**, *16*, 339–346.

[58] D. Chen, M. Mauk, X. Qiu, C. Liu, J. Kim, S. Ramprasad, S. Ongagna, W. R. Abrams, D. Malamud, P. L. A. M. Corstjens, et al., *Biomed. Microdevices* **2010**, *12*, 705–19.

[59] M. Kokoris, M. Nabavi, C. Lancaster, J. Clemmens, P. Maloney, J. Capadanno, J. Gerdes, C. F. Battrell, *Methods* **2005**, *37*, 114–9.

[60] C. H. Setchell, *J. Chem. Technol. Biotechnol., Biotechnol.* **1985**, *35*, 175–182.

[61] B.-I. Haukanes, C. Kvam, *Nat. Biotechnol.* **1993**, *11*, 60–63.

[62] O. Olsvik, T. Popovic, E. Skjerve, K. S. Cudjoe, E. Hornes, J. Ugelstad, M. Uhlen, *Clin. Microbiol. Rev.* **1994**, *7*, 43–54.

[63] K. Aguilar-Arteaga, J. A. Rodriguez, E. Barrado, *Anal. Chim. Acta* **2010**, *674*, 157–65.

[64] G. R. M. Duarte, C. W. Price, B. H. Augustine, E. Carrilho, J. P. Landers, *Anal. Chem.* **2011**, *83*, 5182–9.

[65] K.-Y. Lien, C.-J. Liu, P.-L. Kuo, G.-B. Lee, *Anal. Chem.* **2009**, *81*, 4502–9.

[66] H. Bordelon, N. M. Adams, A. S. Klemm, P. K. Russ, J. V Williams, H. K. Talbot, D. W. Wright, F. R. Haselton, *ACS Appl. Mater. Interfaces* **2011**, *3*, 2161–2168.

[67] U. Lehmann, C. Vandevyver, V. K. Parashar, M. A. M. Gijs, *Angew. Chem.* **2006,** *118*, 3132–7; *Angew. Chem. Int. Ed. Engl.* **2006**, *45*, 3062–7.

[68] K. Sur, S. M. McFall, E. T. Yeh, S. R. Jangam, M. A. Hayden, S. D. Stroupe, D. M. Kelso, *J. Mol. Diagn.* **2010**, *12*, 620–8.

[69] C. Liu, K. Lien, C. Weng, J.-W. Shin, T.-Y. Chang, G.-B. Lee, *Biomed. Microdevices* **2009**, *11*, 339–350.

[70] K.-Y. Lien, C.-J. Liu, Y.-C. Lin, P.-L. Kuo, G.-B. Lee, *Microfluid. Nanofluid.* **2008**, *6*, 539–555.

[71] D. Liu, G. Liang, Q. Zhang, B. Chen, *Anal. Chem.* **2013**, *85*, 4698–4704.

[72] S. J. Reinholt, A. Behrent, C. Greene, A. Kalfe, and A. J. Baeumner, Isolation and Amplification of mRNA within a Microfluidic Lab on a Chip, *Anal. Chem.* **2013,** accepted 12/2/2013 in press.

[73] G. Jiang, D. J. Harrison, *Analyst* **2000**, *125*, 2176–2179.

[74] J. S. Marcus, W. F. Anderson, S. R. Quake, *Anal. Chem.* **2006**, *78*, 3084–9.

[75] S. M. Berry, E. T. Alarid, D. J. Beebe, *Lab Chip* **2011**, *11*, 1747–53.

[76] S. W. Yeung, I.-M. Hsing, *Biosens. Bioelectron.* **2006**, *21*, 989–97.

[77] J. Wang, K. Morabito, J. X. Tang, A. Tripathi, *Biomicrofluidics* **2013**, *7*, 044107–1–044107–12.

[78] C.-H. Wang, K.-Y. Lien, T.-Y. Wang, T.-Y. Chen, G.-B. Lee, *Biosens. Bioelectron.* **2011**, *26*, 2045–52.

[79] C.-H. Wang, K.-Y. Lien, J.-J. Wu, G.-B. Lee, *Lab Chip* **2011**, *11*, 1521–31.

[80] C.-H. Wang, K.-Y. Lien, L.-Y. Hung, H.-Y. Lei, G.-B. Lee, *Microfluid. Nanofluid.* **2012**, *13*, 113–123.

[81] M. B. Esch, L. E. Locascio, M. J. Tarlov, R. A. Durst, *Anal. Chem.* **2001**, *73*, 2952–8.

[82] B. C. Satterfield, S. Stern, M. R. Caplan, K. W. Hukari, J. A. A. West, *Anal. Chem.* **2007**, *79*, 6230–5.

[83] B. E. Root, A. K. Agarwal, D. M. Kelso, A. E. Barron, *Anal. Chem.* **2011**, *83*, 982–8.

[84] K. A. Hagan, W. L. Meier, J. P. Ferrance, J. P. Landers, *Anal. Chem.* **2009**, *81*, 5249–56.

[85] W. Cao, C. J. Easley, J. P. Ferrance, J. P. Landers, *Anal. Chem.* **2006**, *78*, 7222–8.

[86] K. A. Hagan, C. R. Reedy, M. L. Uchimoto, D. Basu, D. A. Engel, J. P. Landers, *Lab Chip* **2011**, *11*, 957–61.

[87] J. Kim, M. Mauk, D. Chen, X. Qiu, J. Kim, B. Gale, H. H. Bau, *Analyst* **2010**, *135*, 2408–14.

[88] E. A. Oblath, W. H. Henley, J. P. Alarie, J. M. Ramsey, *Lab Chip* **2013**, 13, 1325–32.

[89] T. L. Hawkins, T. O'Connor-Morin, A. Roy, C. Santillan, *Nucleic Acids Res.* **1994**, *22*, 4543–4.

[90] M. A. Witek, M. L. Hupert, D. S.-W. Park, K. Fears, M. C. Murphy, S. A. Soper, *Anal. Chem.* **2008**, *80*, 3483–91.

[91] Y. Xu, B. Vaidya, A. B. Patel, S. M. Ford, R. L. McCarley, S. A. Soper, *Anal. Chem.* **2003**, *75*, 2975–84.

[92] M. A. Witek, S. D. Llopis, A. Wheatley, R. L. McCarley, S. A. Soper, *Nucleic Acids Res.* **2006**, *34*, e74.

[93] D. S.-W. Park, M. L. Hupert, M. A. Witek, B. H. You, P. Datta, J. Guy, J.-B. Lee, S. A. Soper, D. E. Nikitopoulos, M. C. Murphy, *Biomed. Microdevices* **2008**, *10*, 21–33.

[94] T. Nakagawa, T. Tanaka, D. Niwa, T. Osaka, H. Takeyama, T. Matsunaga, *J. Biotechnol.* **2005**, *116*, 105–11.

[95] A. Persat, L. A. Marshall, J. G. Santiago, *Anal. Chem.* **2009**, *81*, 9507–9511.

[96] L. A. Marshall, L. L. Wu, S. Babikian, M. Bachman, J. G. Santiago, *Anal. Chem.* **2012**, *84*, 9640–5.

[97] Y. Huang, S. Joo, M. Duhon, M. Heller, B. Wallace, X. Xu, *Anal. Chem.* **2002**, *74*, 3362–71.

[98] C. Prinz, J. O. Tegenfeldt, R. H. Austin, E. C. Cox, J. C. Sturm, *Lab Chip* **2002**, *2*, 207–12.

[99] P. Vulto, G. Dame, U. Maier, S. Makohliso, S. Podszun, P. Zahn, G. A. Urban, *Lab Chip* **2010**, *10*, 610–6.

[100] B. M. Olivera, P. Baine, N. Davidson, *Biopolymers* **1964**, *2*, 245–257.

[101] R. Zhang, H.-Q. Gong, X. Zeng, C. Lou, C. Sze, *Anal. Chem.* **2013**, *85*, 1484–91.

CHAPTER 2

ISOLATION AND AMPLIFICATION OF mRNA WITHIN A MICROFLUIDIC LAB ON A CHIP[1]

Abstract

The major modules for realizing molecular biological assays in a micro total analysis system (μTAS) were developed for the detection of pathogenic organisms. The specific focus was the isolation and amplification of eukaryotic messenger RNA (mRNA) within a simple, single-channel device for very low RNA concentrations that could then be integrated with detection modules. The *hsp70* mRNA from *Cryptosporidium parvum* was used as a model analyte. Important points of study were surface chemistries within poly(methyl methacrylate) (PMMA) microfluidic channels that enabled specific and sensitive mRNA isolation and amplification reactions for very low mRNA concentrations. Optimal conditions were achieved when the channel surface was carboxylated via UV/ozone treatment followed by the immobilization of polyamidoamine (PAMAM) dendrimers on the surface, thus increasing the immobilization efficiency of the thymidine oligonucleotide, oligo$(dT)_{25}$, and providing a reliable surface for the amplification reaction, importantly, without the need for blocking agents. Additional chemical modifications of the remaining active surface groups were studied to avoid non-specific capturing of nucleic acids and hindering of the mRNA amplification at low RNA concentrations. Amplification of the mRNA was accomplished using nucleic acid sequence-based amplification (NASBA), an isothermal, primer-dependent technique. Positive controls consisting of previously generated NASBA

[1] This section has been reproduced, with modifications to conform to the required format, with permission from Analytical Chemistry, in press. Unpublished work copyright 2013 American Chemical Society. S. J. Reinholt, A. Behrent, C. Greene, A. Kalfe, A. J. Baeumner, *Anal. Chem.* **2013**, DOI 10.1021/ac403417z.

amplicons could be diluted 10^{15} fold and still result in successful on-chip re-amplification. Finally, the successful isolation and amplification of mRNA from as few as 30 *C. parvum* oocysts was demonstrated directly on-chip and compared to bench-top devices. This is the first proof of successful mRNA isolation and NASBA-based amplification of mRNA within a simple microfluidic device in relevant analytical volumes.

1 Introduction

Rapid and reliable detection of microorganisms is essential for useful applications in areas such as food safety, water quality, clinical analysis, and defense against bioterrorism. Traditional microbiological methods requiring the use of culturing techniques are time-consuming, and only applicable to organisms that can be grown under laboratory conditions. For these reasons, when possible, they have been replaced by techniques that involve polymerase chain reaction (PCR) with real-time detection as these assays are highly specific, highly sensitive, and very rapid needing only hours instead of days to produce a conclusive result.[1-5]

Portability of these assays is also very advantageous and allows for onsite, or point-of-care, testing, which further decreases the time and cost of acquiring results. The concept of a micro total analysis system (μTAS), later indicated as a lab on a chip, was introduced by Manz *et al.* in the early 1990s.[6,7] They proposed scaling down the size of chemical analytical devices to improve performance. An ideal μTAS requires only a small volume of sample and incorporates all necessary manipulation and analysis steps to deliver a quantitative, or in some cases qualitative, result in a simple sample-in-answer-out fashion. The μTAS concept has also been applied to biological assays, including the detection of microorganisms within microfluidic devices, and many of these systems have successfully incorporated PCR into the design.[1-5] As the temperature

cycling necessary in PCR greatly increases the complexity of devices that incorporate this method of amplification, isothermal amplification processes have been explored. Amplification techniques, such as helicase-dependent amplification (HDA),[8,9] loop-mediated isothermal amplification (LAMP),[10-12] rolling circle amplification (RCA),[13,14] and nucleic acid sequence-based amplification (NASBA),[15-18] have been integrated into μTAS designs, offering decreased chip complexity as there is no need for temperature cycling equipment. NASBA is a primer-dependent amplification technique that is able to amplify single-stranded RNA.[19] Specifically, this process uses T7 RNA polymerase, RNaseH, avian myeloblastosis virus (AMV) reverse transcriptase, two primers specific to the target sequence, deoxynucleoside triphosphates (dNTPs), and buffers to facilitate a cyclic amplification reaction at a constant temperature that is capable of producing a 10^9-fold amplification in 90-120 minutes.[19] NASBA was the amplification technique used in this study.

Many of these microanalytical systems that incorporate nucleic acid amplification use glass-, silicon- and quartz-based devices.[20] However, the fabrication of these microchips is often expensive and time-consuming.[20] Consequently, organic polymers have been used as an alternative.[3,9,10,15,17,18,21-27] Poly(methyl methacrylate) (PMMA) is a commonly used substrate for microfluidic device fabrication due to its advantageous properties, including its machinability, low cost, and optical transparency,[20,28] and it was explored as a new material for NASBA in this study.

Within microfluidic devices, silica structures/beads[15,29-31] and paramagnetic beads[32,33] are often used for nucleic acid isolation from a lysate sample. However, these methods require increased microdevice complexity, are more complicated to use, and are expensive. Furthermore, the previous microdevice that incorporated both nucleic acid isolation and NASBA had separate chambers for isolation and NASBA,[15] making the device more complex to fabricate and use as

well as increase the potential loss of target nucleic acids during transfer, which is especially a problem at low RNA concentrations. Here, we present a very simple single-microchannel design that uses surface chemistry to facilitate both the nucleic acid isolation and NASBA.

The protozoan parasite, *Cryptosporidium parvum* (*C. parvum*), is an organism of interest in the water quality community due to its highly infective nature in humans and other mammals.[34,35] This pathogen causes the disease, cryptosporidiosis, which is a gastrointestinal disease that is potentially fatal in immunocompromised and immunosuppressed patients.[34,35] This parasite is of concern in countries relying on chlorination as a form of water treatment as it is ineffective when *C. parvum* is in its oocyst state.[34,35] Due to the worldwide importance of *C. parvum* detection, it was chosen as the model analyte for our μTAS.

In this study, we present a PMMA microfluidic device that is capable of isolating and amplifying specific messenger RNA (mRNA) from lysed *C. parvum* oocyst samples. Specifically, mRNA is targeted to differentiate between and only detect viable oocysts, since dead oocysts are not infectious.[36] The microchannels undergo surface chemistry modifications to enable mRNA isolation directly on the channel surface, and amplification via NASBA is performed within the same channel. Surface modifications of the channels were studied to determine an optimal surface for both mRNA isolation and amplification, avoid non-specific binding of proteins and nucleic acids, and hence prevent loss of NASBA enzymes and increase availability of the mRNA to these enzymes.

2 Experimental Methods

2.1 Microfluidic Channel Fabrication

Microfluidic channels were patterned simply and rapidly in PMMA (Lucite Int., UK) via a hot embossing technique using a copper template as previously described.[25] The copper template was fabricated at the Cornell Nanoscale Facility (CNF) via photolithography using KMPR 1050 (Micro-Chem Corp., MA) and copper electroplating resulting in elevated channel structures. A 5x5cm piece of PMMA was sandwiched between the copper template and a blank copper plate, and using a hot press (CarverLaminating), the PMMA was patterned at 130°C and 8000 lbs. of pressure for 10 minutes. Inlet and outlet holes were drilled in the embossed piece of PMMA. The device was bonded similarly to that previously described using UV/ozone-assisted thermal bonding.[37] The embossed PMMA and a second 5x5cm piece of blank PMMA were UV/ozone-treated for 10 minutes using a UVO-Cleaner (Model 144AX, Jelight Company Inc, Irvine, USA). This treatment decreases the glass transition temperature of the surface only, which ensures bonding of the channels without channel deformation.[37] They were then sandwiched between two blank copper plates, and pressed at 90°C and 5000 lbs. of pressure for 10 minutes. Tygon tubing (S-54-HL, Murdock Industrial) with an inner diameter of 0.010" and outer diameter of 0.030" was glued at the inlet and outlet holes of the channels to allow connection to 1mL syringes (Becton, Dickinson and Company) with 30-gauge, luer lock, blunted, stainless-steel needles (Small Parts, Inc.). After fabrication, the chips were stored dry, and typically used the following day. Prior to any surface chemistry, nuclease-free water was pumped into the channels by hand at a high flow rate to expel all the air and ensure no bubble trapping occurred, as well as to test for leakage. Figure 2.1 shows a completely assembled microfluidic device consisting of 6 microchannels each with a

volume of approximately 3.5µL, as well as a schematic representation of the mRNA isolation and NASBA within the microchannels with surface chemistry modifications described below.

2.2 Surface Chemistry Modification

The UV/ozone treatment, prior to bonding, chemically modified the surface of the PMMA resulting in a carboxylated surface,[38] which facilitated the surface chemistry modifications for mRNA isolation. Polyamidoamine (PAMAM) dendrimers (Dendritech Inc.) were immobilized on

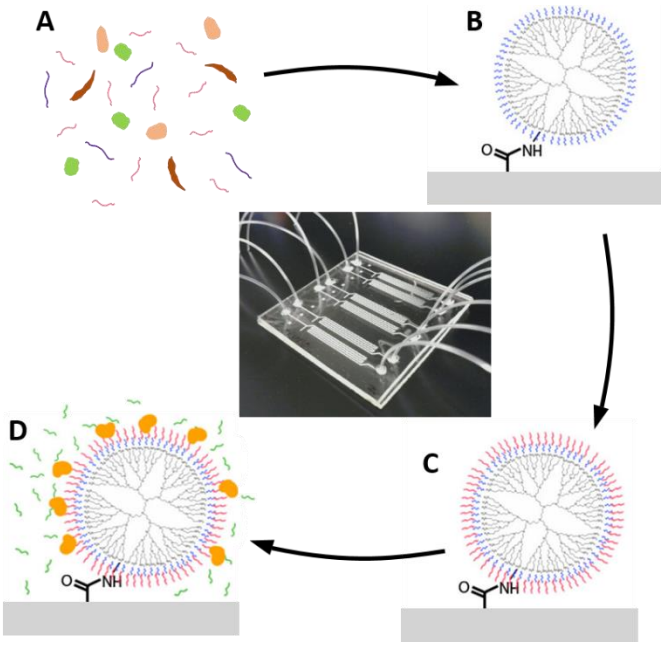

Figure 2.1: Image of a completed 6-channel microfluidic device and a step-by-step schematic of the isolation and NASBA process within the microchannels. A sample of C. parvum lysate with the target mRNA (A) flows into the surface-modified microchannel (B), where the mRNA is isolated (C). NASBA reagents are injected into the microchannel, and the target mRNA is amplified (D).

the channel surface to ultimately increase the immobilization efficiency of oligomer probes.[39] The PAMAM dendrimers used were 5th generation dendrimers, which possess 128 amine surface groups, and they were immobilized using 1-Ethyl-3-(3-dimethylaminopropyl) carbodiimide

hydrochloride (EDC)/N-Hydroxysuccinimide (NHS) crosslinking chemistry. This was accomplished by flowing 150µL of solution (200mM EDC (Sigma Aldrich), 200mM NHS (Thermo Scientific), and 500mM NaCl (Sigma Aldrich) in 50mM 2-(N-Morpholino)ethanesulfonic acid (MES) (FisherBiotech) pH 6.0) through the channels at 5µL/min using a syringe pump (KD Scientific, MA). EDC initially reacts with the carboxylic acid groups on the channel surface, and then it is replaced by NHS to form a more stable NHS-ester that readily reacts with amine groups. Immediately following the EDC/NHS reaction, 150µL of 2mM PAMAM dendrimers in a solution of 10mM NaCl and 50mM N-(2-Hydroxyethyl)piperazine-N'-2-ethanesulfonic acid (HEPES) (Mallinckrodt Baker) pH 8.5 were pumped through the channels at 1µL/min and allowed to incubate at room temperature overnight. The channels were then rinsed with 200µL of nuclease-free water (BDH) at 20µL/min. Phosphate-modified thymidine oligonucleotides, 5'-[Phos]-$[T]_{25}$-3' ([Phos]-oligo$(dT)_{25}$) (Eurofins MWG Operon) were then immobilized on the periphery of the dendrimers using EDC as a crosslinker. Here, 150µL of solution (60µM [Phos]-oligo$(dT)_{25}$, 200mM EDC, and 100mM imidazole (Sigma Aldrich) in nuclease-free water) were pumped through the channels at 1µL/min and again allowed to incubate overnight at room temperature.

The remaining unmodified amine groups on the dendrimers were subsequently modified to eliminate the positive charges that resulted from the amine groups. Without this modification, the amine groups would attract the negatively charged DNA and RNA molecules to the surface and render them unavailable to the NASBA enzymes. The unmodified amine groups were converted to carboxylic acid groups via succinic anhydride modification. A solution of 200mM succinic anhydride (Alfa Aesar) in 700mM borate buffer adjusted to pH 9 was used, and 200µL were pumped through the channels at 20µL/min. This was followed by a 200µL wash with 1M 2-

Amino-2-hydroxymethyl-propane-1,3-diol (Tris)-HCL (Sigma Aldrich) adjusted to pH 9 pumped through the channels at 20μL/min. The channels were then rinsed by pumping 200μL of nuclease-free water at 20μL/min. The microfluidic channels were then ready to be used for *C. parvum* isolation and amplification.

2.3 Evaluation of Surface Chemistry Modifications

To evaluate carboxylation density on the channel surface after UV/ozone treatment, an assay using Toluidine Blue O (TBO) (TCI America) was performed. TBO is a dye that adsorbs to carboxylic groups in an alkaline environment and desorbs in acidic conditions.[40] After bonding the channels, 200μL of 500μM TBO in deionized water adjusted to pH 10 were pumped through the channels at 20μL/min, which caused the TBO to adsorb. The channels were washed with 200μL of deionized water adjusted to pH 10 at 20μL/min. Finally, 150μL of 50% (w/w) acetic acid were pumped through the channels at 20μL/min to cause desorption of the TBO, and the effluent was collected in a 96-well microtiter plate. The absorption at 633 nm was measured using a PowerWave XS plate reader (BioTek Instruments Inc.).

An Acid Orange 7 (AO7) assay[41] was used to assess the density of amine groups, and therefore of dendrimers immobilized on the surface of the channels. The assay is analogous to the TBO assay described above. A solution of 1mM AO7 (TCI America) in deionized water adjusted to pH 3 was pumped into the channels and washed with deionized-water at pH 3. The dye was desorbed with deionized water adjusted to pH 12 and collected in a 96-well microtiter plate. Flow rates and volumes were the same as described for the TBO assay above. The absorption was measured at 460 nm using a plate reader.

The immobilization efficiency of oligo$(dT)_{25}$ on a dendrimer-modified surface was compared to that on a simple carboxylated surface by measuring its capture efficiency of a fluorescent complimentary adenosine oligonucleotide, oligo$(dA)_{25}$. For this comparison, amine-modified oligo$(dT)_{25}$ probes were immobilized onto the carboxylated microchannel surface (no dendrimers) using EDC as a crosslinker, and this was done by pumping the EDC/NHS solution through the channels as described above, and then pumping 150µL of 60µM [NH_2]-oligo$(dT)_{25}$ and 10mM NaCl in 50mM HEPES at pH 8.5 through the channels at 1µl/min and allowing incubation overnight at room temperature. Fluorescein-conjugated oligo$(dA)_{25}$ was prepared at 10µM in nuclease-free water, and 100µL were pumped through both types of modified channels at 5µL/min. The excess oligo$(dA)_{25}$ was washed out of the channels using 30µL of washing buffer B (Invitrogen Dynabeads Kit) at 1µL/min. The channels were placed on a heating block set at 82°C, 150µL of 0.01M Tris-HCl at pH 7.5 was pumped through the channel at 20µL/min, and the effluent from each channel was collected in a 96-well microtiter plate. The fluorescence was measured using an FLx800 fluorescence plate reader (BioTek Instruments Inc.) at an absorbance wavelength of 485nm and an emission wavelength of 528nm. Carboxylated channels and dendrimer-modified channels without oligo$(dT)_{25}$ were also tested as negative controls.

2.4 Heat Shock and Lysis

Live *C. parvum* oocysts in 1x phosphate-buffered saline (1xPBS) were obtained from Waterborne Inc., and diluted to concentrations of interest using nuclease-free water. The oocyst samples were heat-shocked in a heating block at 41°C for 5 minutes to cause a high transcription yield of the target, *heat-shock protein 70* (*hsp70*) mRNA. The oocysts samples were subsequently diluted in Lysis Binding Buffer (Invitrogen Dynabeads Kit) and lysed via five repeated freeze-thaw cycles. The samples were stored at -80°C until needed.

2.5 mRNA Isolation within the Microchannels

A volume of 150µL of *C. parvum* lysate was pumped through the channels at 5µL/min. This allowed any mRNA in the sample to hybridize with the immobilized oligo$(dT)_{25}$ via its poly-adenosine (poly-A) tail. Several different washing techniques were tested to clear the cellular debris, proteins, unbound nucleic acids, and lysis binding buffer out of the channels without washing out the desired target mRNA. The optimal washing parameters were to pump 100µL of washing buffer B (Invitrogen Dynabeads Kit) through the channels at 5µL/min and then 50µL of nuclease-free water at 5µL/min. Finishing the washing steps with nuclease-free water is necessary as many buffers including the lysis binding buffer and washing buffer B inhibited NASBA. Bench top controls for the isolation procedure were performed in Eppendorf tubes (VWR) using paramagnetic beads coated with oligo$(dT)_{25}$ according to the manufacturer's instruction in the Dynabeads® mRNA DIRECT™ Micro Kit (Invitrogen).

2.6 NASBA within the Microchannels

The NASBA solution consisting of enzymes, primers, and dNTPs was prepared using the NucliSENS Easy-Q Basic Kit (BioMérieux, USA) according to the manufacturer's instructions. The sequences for both primers can be seen in Table 2.1. This solution was pumped into the channels by hand until the microchannels were completely filled. The microchannels were then submerged in a water bath set at 41°C for 90 minutes with gentle manual agitation every 30 minutes. Following incubation, the samples were expelled from the channels into Eppendorf tubes for off-chip detection. Positive NASBA controls were samples of NASBA amplicon diluted $1{:}10^8$ in nuclease-free water. Negative NASBA controls were samples containing only nuclease-free water. These controls underwent NASBA on the bench top where the NASBA reagents and

enzymes were added directly to the Eppendorf tube and incubated in a water bath at 41°C for 90 minutes. Controls accounting for cross-reactivity with other microorganisms were perform previously,[42] and here, the specificity of the assay to *C. parvum* was confirmed.

2.7 Lateral Flow Assay

A lateral flow assay (LFA) was used to detect any *C. parvum* target sequences in the sample solution.[35] These assays used sulforhodamine B (SRB)-encapsulating liposomes tagged with *C. parvum* reporter probe (Table 2.1) that were synthesized as previously described.[43] A 1µL volume of sample solution was mixed with 1µL of liposomes, 1µL of 1x HEPES sucrose saline (1xHSS), and 5µL of hybridization buffer (20% formamide, 4x saline sodium citrate (4XSSC), 0.2% Ficoll type 400, and 125mM sucrose), and this solution was incubated at 41°C for 5 minutes to allow any target sequences to hybridize with the reporter probes conjugated to the liposomes. These samples were allowed to vertically flow up nitrocellulose strips containing immobilized *C. parvum* capture probes (Table 2.1). Samples containing target sequences formed sandwich hybridizations that produced a colorimetric signal. The LFA signals were evaluated visually and scanned using a flatbed scanner. ImageJ software was then used for quantification of the obtained signal intensities. This approach was chosen over analyses via a reflectometer[44] as the probing surface would not have covered the entire strip surface in the latter approach.

Table 2.1: *C. parvum*-associated Sequences[42]

DNA Probe/Primer	**Sequence 5'-3'**
NASBA Primer 1	AATTCTAATACGACTCACTATAGGGAGAAGGTAGAACCACC AACCAATACA
NASBA Primer 2	AGATTCGAAGAACTCTGCGCTGA
Reporter Probe	GTGCAACTTTAGCTCCAGTT
Capture Probe	AGATTCGAACTCTGCGC

The entire assay for *C. parvum* detection takes approximately 3 hours from heat shock to colorimetric signal detection via lateral flow assay.

3 Results and Discussion

The ultimate goal of the presented studies was to combine isolation and amplification of mRNA molecules into a single inexpensive, simple, polymer-based microfluidic device. Previously, there has only been one demonstration of nucleic acid isolation and NASBA within the same microchip[15] to our knowledge, and here, solid-phase extraction via silica beads was used for nucleic acid isolation. This nucleic acid isolation technique increases chip complexity, decreases ease of use, and non-specifically binds all nucleic acids using chaotropic salts and organic solvents that inhibit NASBA. Thus, an exploration of surface modifications within the microfluidic channels to facilitate mRNA isolation was performed to realize an efficient capture method while avoiding non-specific binding and denaturing of NASBA enzymes.

3.1 Microfluidic Channel Fabrication

The use of PMMA as the substrate material has several advantages. PMMA is inexpensive, durable, very easy and inexpensive to pattern, and easily facilitates the surface chemistry for mRNA isolation. Our extremely simple single-channel design is also very beneficial. Unlike the previous design that contained separate chambers for nucleic acid isolation and amplification, our design enables simple fabrication and operation as well as the elimination of losses due to nucleic acid transfer between the isolation and amplification modules, which is especially critical for low RNA concentrations. Additionally, each chip contains six parallel microchannels that enable six samples to be processed in parallel on a single chip demonstrating the ability for multiplexing with our design.

3.2 Surface Chemistry Modification

In order to render the PMMA surface chemically active, carboxylic acid groups were generated using UV/ozone treatment, which were subsequently changed to amine groups using PAMAM dendrimers. The density of carboxylic acid groups after UV/ozone treatment and amine groups after dendrimer immobilization on the surface of the channel was measured using simple dye assays for an initial assessment of the success of the modification. TBO assays determined the carboxylic acid density to be between 5 and 33 nmol/cm², with a relative standard deviation (RSD) up to 33%. AO7 assays were used to measure the amine-group density after channels were coated with PAMAM dendrimers and values between 70 and 105 nmol/cm² were obtained. The RSD was between 3 and 26% for channels within the same experiment, and 20% between experiments. While being simple methods, they provided a reasonable and rapid indication of the desired surface modifications, which were then further used and more quantitatively analyzed as described below. Most importantly, it was determined that the use of PAMAM dendrimers provides a significant increase in the number of available functional group as compared to simple UV/ozone functionalization alone.

The advantage of using a dendrimer surface was then quantitatively demonstrated by testing the immobilization efficiency of oligo$(dT)_{25}$ and the capture efficiency of oligo$(dA)_{25}$ by immobilized oligo$(dT)_{25}$ on both the carboxylated channel surface and dendrimer-modified channel surface (Figure 2.2). The concentration of oligo$(dT)_{25}$ on the channel surfaces was quantified using fluorescently-labelled oligonucleotides. Here, an 18-fold increase in the number of immobilized oligo$(dT)_{25}$ molecules was found using a dendrimer-modified surface versus a simply carboxylated surface (Figure 2.2a). This dramatic difference was still apparent when evaluating the actual hybridization functionality of the immobilized oligonucleotides. Here,

fluorescently-labelled oligo$(dA)_{25}$ was allowed to hybridize with the immobilized oligo$(dT)_{25}$ capture probes. The dendrimer-modified surface resulted in a 16-fold increase in capture efficiency relative to the carboxylated surface (Figure 2.2b). Consequently, all of the channels used for mRNA isolation had dendrimer-modified surfaces.

In previous reports of microfluidic NASBA, blocking of the device surface using BSA or yeast tRNA was necessary to prevent non-specific adsorption of the NASBA enzymes.[15-18] This requires additional steps, which can increase the overall assay time, or if added to the NASBA mixture can present potential interferents, which can affect NASBA. However, blocking agents are not necessary in the device presented here; the surface modifications necessary for efficient and simple mRNA isolation provide a suitable surface for NASBA, making it therefore a significantly more robust device.

3.3 mRNA Isolation within the Microchannels

Initially, isolation of the mRNA from lysed *C. parvum* oocyst samples within the functionalized channels was demonstrated independently from an on-chip NASBA reaction. Here, following the on-chip mRNA isolation procedure, the captured mRNA was dehybridized and expelled from the channels into Eppendorf tubes by pumping 20µL of nuclease-free water at 20µL/min while the channels were submerged in a water bath at 65°C. The NASBA reaction solution was then added to each tube and they were incubated in a water bath at 41°C for 90 minutes following conditions previously published for *C. parvum hsp70* mRNA.[45] It was quickly determined that only the surfaces containing the dendrimers enabled a truly reliable and successful mRNA isolation. While some success was also obtained with carboxylated surfaces, the dendrimer-modified surface proved to be more reliable for both mRNA isolation and amplification

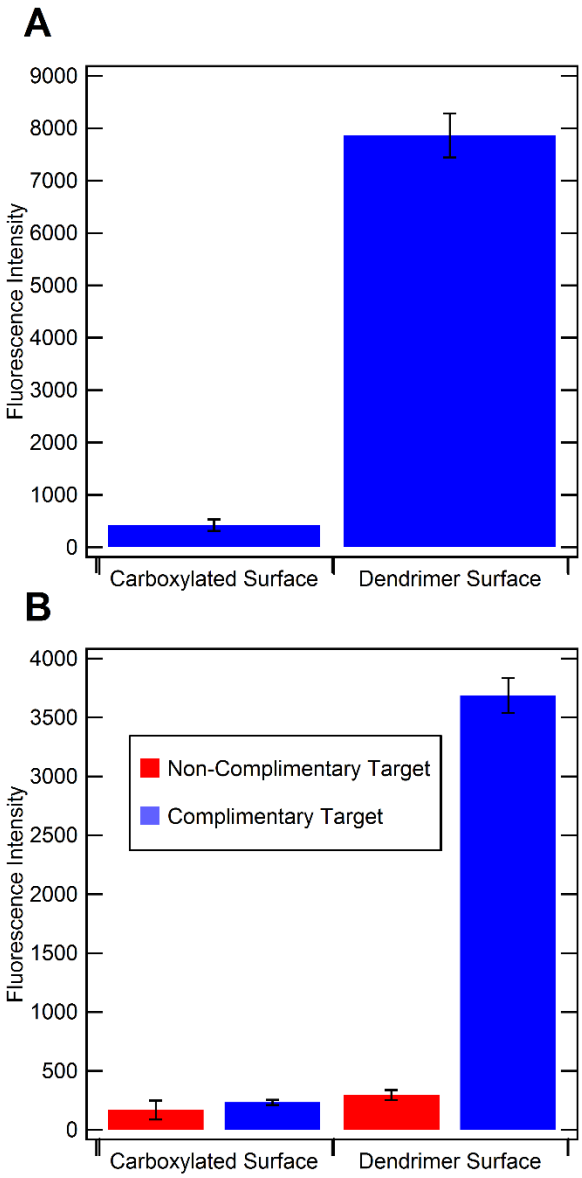

Figure 2.2: Comparison of oligo(dT)$_{25}$ immobilization efficiency and oligo(dA)$_{25}$ capture efficiency by oligo(dT)$_{25}$ on carboxylated channel surfaces and dendrimer-modified channel surfaces. Fluroescently-labelled oligo(dT)$_{25}$ was immobilized on carboxylated surfaces containing no dendrimers and dendrimer-modified surfaces, and the fluorescence intensities were compared for the different surfaces (A). Fluorescently-labelled oligo(dA)$_{25}$ (complimentary target) was captured on both carboxylated and dendrimer-modified surfaces with immobilized oligo(dT)$_{25}$ capture probes, and the fluorescence was quantified (B: blue bars). Fluorescent oligo(dT)$_{25}$ (non-complimentary target) was also pumped through both of these channels to determine the non-specific binding to each type of surface (B: red bars).

within the same channel. Here, when challenging the procedure to low analyte concentrations, successful mRNA isolation could be demonstrated for as few as 10 and 50 oocysts (Figure 2.3).

Signals obtained are lower than that of the positive control (a 1:10^8 dilution of positive NASBA amplicon) as a low mRNA concentration is to be expected from 10 and 50 oocysts, since the RNA was highly diluted when expelled from the microfluidic channel (into a 20µL, instead of 5µL, volume) and because we assume that isolation and dehybridization reactions did not provide a 100% yield.

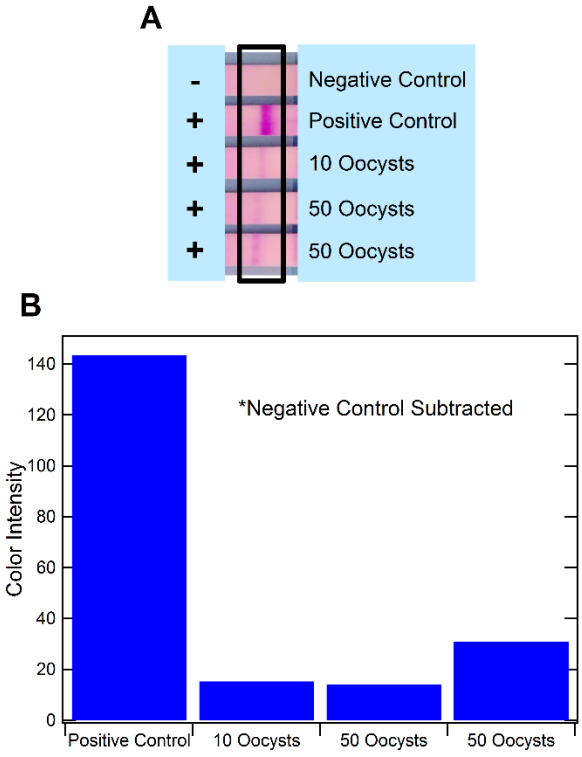

Figure 2.3: Results from mRNA isolation within the microchannels and bench top NASBA. The results of on-chip isolation and off-chip NASBA for 10 and 50 *C. parvum* oocysts are shown by the LFA strips (A). An ImageJ quantification of the color intensity of the strips is also shown (B). The positive control is NASBA amplicon diluted by 10^8.

3.4 NASBA within the Microchannels

Secondly, NASBA was realized within the microchannels separately from mRNA isolation from lysed oocysts. Initially, a set-up was determined that would result in a temperature-controlled environment to ensure appropriate NASBA conditions. While ultimately an internal heating

element will be desirable, a water bath was chosen to avoid temperature fluctuations and facilitate easy access to the microfluidic channel for desired manipulations. The seal achieved through the device fabrication ensured a no-leakage set up. Samples chosen initially were dilutions of NASBA amplicons. In the bench top positive control, the amplicon is diluted by a factor of 10^8. For assessing NASBA within the channels, dilutions of 10^{10}, 10^{11}, 10^{13}, and 10^{15} were tested. These samples were mixed with the NASBA reaction solution and pumped into the channels. The channels were then incubated at 41°C for 90 minutes with gentle agitation every 30 minutes. Initial experiments were carried out in microfluidic channels with varying surface chemistries including carboxylic acid groups, dendrimers (amine groups), as well as dendrimer surfaces blocked with 0.01-1% (w/v) polyvinyl pyrrolidone, 0.1-1% (w/v) bovine serum albumin (BSA), 0.01-1% (w/v) gelatin, and 1.11-111ng of extracted *Escherichia coli* (*E. coli*) RNA. However, in all of these cases only insufficient or unreliable amplification was observed. It was assumed that enzyme adsorption to the channels and/or loss of mRNA through non-specific binding led to unsuccessful amplification reactions.

General protein adsorption to the channel surface (and possibly Tygon tubing) was therefore determined through a model protein, horseradish peroxidase (HRP). Here, a 0.1µg/mL concentration of HRP was pumped through the microfluidic channel and the activity was determined in the outflow. However, the possible loss that may have occurred in the channels could not be differentiated from the original solution. It was therefore assumed that inaccessibility of mRNA molecules for NASBA amplification was likely the main challenge. Thus, the dendrimers' peripheral amine groups were modified using succinic anhydride to convert the amine groups to carboxylic acid groups. This provided repelling surfaces for mRNA molecules and assisted in achieving an appropriate pH of approximately 8.5 for the NASBA reaction. When

utilizing this optimized dendrimer surface coupled to oligo(dT)$_{25}$ capture probes, highly reliable and sensitive amplification could be realized (Figure 2.4). The dilution of the positive NASBA amplicon to 10^{15} is pushing the limit of RNA molecules present in a sample as NASBA typically provides a 10^{9} – 10^{11}-fold amplification of RNA molecules.[46] Thus, on-chip NASBA was demonstrated to be highly successful and could now be combined with on-chip mRNA isolation.

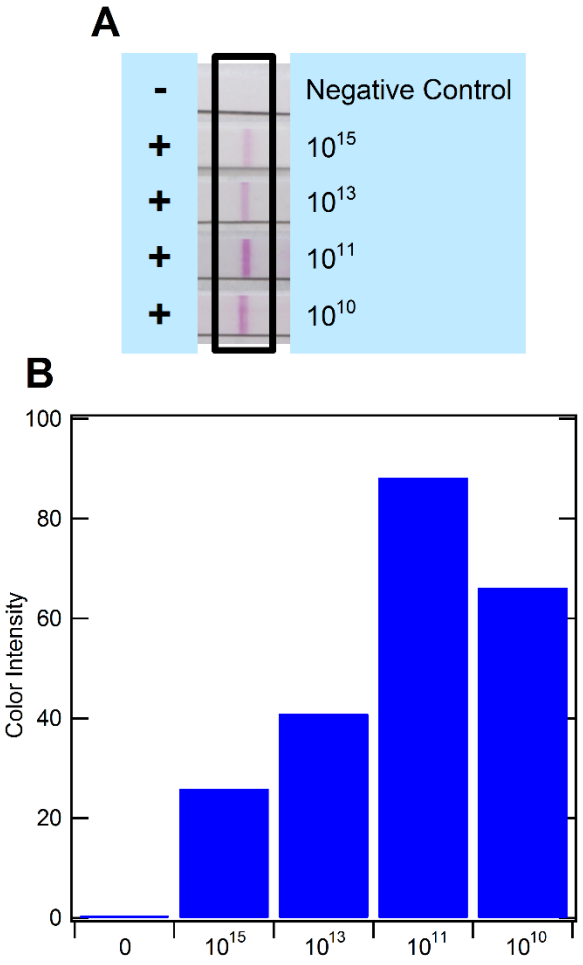

Figure 2.4: Results from NASBA within microchannels using diluted amplicon. The results of on-chip NASBA for amplicon dilutions of 10^{10}-10^{15} are shown by the LFA strips (A). An ImageJ quantification of the color intensity of the strips is also shown (B). The negative control is a sample of nuclease-free water (no amplicon) that underwent NASBA.

3.5 mRNA Isolation and NASBA within the Microchannels

Finally, on-chip isolation of *hsp70* mRNA from lysed *C. parvum* oocyst samples with subsequent on-chip NASBA was successfully demonstrated in the functionalized microfluidic channels within the same device. Various assay conditions were investigated including different washing volumes, flow rates, and buffers. It was found that these factors highly influenced the reliability of the on-chip isolation and NASBA reaction once the dendrimer-oligo$(dT)_{25}$ surface was optimized. Chaotropic salts and organic compounds in the lysis buffer and washing buffer needed to be removed from the microfluidic channels prior to realizing a successful NASBA reaction. At the same time, captured mRNA needed to remain hybridized on the dendrimer-oligo$(dT)_{25}$ surface and accessible for NASBA enzymes and primer binding. In the end, the most reproducible results were obtained by washing with 100µL of washing buffer B at 5µL/min, and then 50µL of nuclease-free water at 5µL/min. On-chip isolation and on-chip amplification of mRNA from just 30 oocysts was successfully demonstrated (Figure 2.5). These results are a significant improvement over the limit of detection reported in the previous microfluidic device incorporating nucleic acid isolation and NASBA, where detection of 100 *Escherichia coli* cells was reported.[15] This suggests an increased performance using surface modifications for nucleic acid purifications over solid-phase isolation as well as a single isolation and amplification chamber to eliminate nucleic acid losses during transport to the amplification chamber. In fact, we have determined that isolation and amplification of higher concentrations of cells (data not shown) demands less defined surface conditions, and leads to easier success, although working at very low RNA (and cell) concentrations requires additional attention. In addition, the dendrimer surface provided a highly reliable surface for avoiding false negative results.

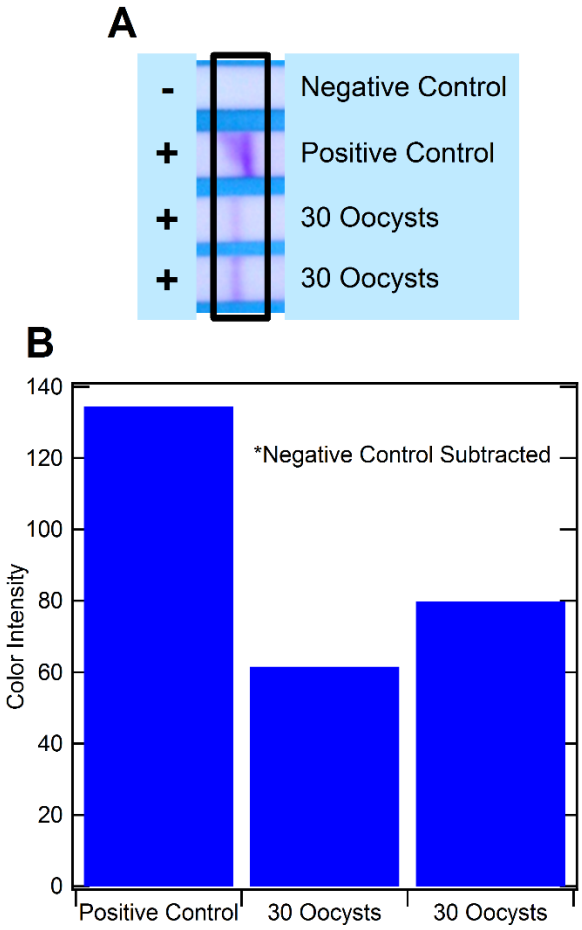

Figure 2.5: Results from mRNA isolation and NASBA within the microfluidic channels. The results of on-chip mRNA isolation and NASBA for *C. parvum* lysate are shown by the LFA strips (A). An ImageJ quantification of the color intensity of the strips is also shown (B). The negative control for NASBA is a sample of nuclease-free water.

4 Conclusion

In biological and chemical analysis, μTASs are increasingly becoming the end goal of developing assays for on-site and point-of-care use. The portability and simplicity of these devices is crucial if they are to be used in resource-limited areas and in situations where experts are not readily available. In this study, we have presented a simple PMMA-based microfluidic device that can isolate and amplify *C. parvum* mRNA from lysed oocysts through surface chemistry modifications and NASBA within the same channel. By incorporating PAMAM dendrimers, a

significant increase in the immobilization efficiency of the oligo$(dT)_{25}$ capture probe was achieved, which provided a 16-fold increase in its capture efficiency. The resulting surface also provided a suitable surface for amplification without necessitating the use of blocking reagents that have always been needed with past on-chip NASBA reactions. Through the exploration of different washing regimes, 30 *C. parvum* oocysts were successfully detected, and this represents a significant improvement in detection compared to the previous device incorporating nucleic acid isolation and NASBA. The isolation and amplification steps of the assay are very important and will be central to a complete μTAS for *C. parvum* oocyst detection, which will also incorporate previously developed oocyst lysis (Rheonix Inc.)[47] and electrochemical detection[48] steps. The presented device is envisioned to be a functional module in a μTAS integrating immunomagnetic separation[42] upstream and electrochemical detection[48] downstream of the module. It is therefore designed to be a highly portable device that is inexpensive, due to the materials ($0.22 in material cost) and fabrication methods used, as well as easy to use, due to the designed simplicity of the assay. An example integration of this device is the automated liquid-handling system, such as the fluidic CARD™ platform developed by Rheonix Inc.[47] The proposed system can be used to detect any eukaryotic microorganism through the mRNA isolation mechanism. This is the first demonstration of *C. parvum* mRNA isolation and amplification using NASBA within a very simple microfluidic device. While being a relevant analyte in itself, *C. parvum* is a prime example of a difficult biological analyte that can be detected with high sensitivity in chip-based devices. The combination of isolation and amplification into the same microfluidic channel avoids loss and contamination otherwise obtained in multi-step procedures, and therefore has the potential as an alternative in the bioanalysis of low-concentration analytes.

5 References

[1] P. Belgrader, S. Young, B. Yuan, M. Primeau, L. A. Christel, F. Pourahmadi, M. A. Northrup, *Anal. Chem.* **2001**, *73*, 286–9.

[2] M. A. Northrup, B. Benett, D. Hadley, P. Landre, S. Lehew, J. Richards, P. Stratton, *Anal. Chem.* **1998**, *70*, 918–22.

[3] A. F. Sauer-Budge, P. Mirer, A. Chatterjee, C. M. Klapperich, D. Chargin, A. Sharon, *Lab Chip* **2009**, *9*, 2803–10.

[4] C. Zhang, J. Xu, W. Ma, W. Zheng, *Biotechnol. Adv.* **2006**, *24*, 243–84.

[5] C. Zhang, D. Xing, *Nucleic Acids Res.* **2007**, *35*, 4223–37.

[6] A. Manz, N. Graber, H. M. Widmer, *Sensors Actuators B Chem.* **1990**, *1*, 244–248.

[7] D. R. Reyes, D. Iossifidis, P.-A. Auroux, A. Manz, *Anal. Chem.* **2002**, *74*, 2623–36.

[8] M. Mahalanabis, J. Do, H. ALMuayad, J. Y. Zhang, C. M. Klapperich, *Biomed. Microdevices* **2010**, *12*, 353–9.

[9] N. Ramalingam, T. C. San, T. J. Kai, M. Y. M. Mak, H.-Q. Gong, *Microfluid. Nanofluidics* **2009**, *7*, 325–336.

[10] X. Fang, Y. Liu, J. Kong, X. Jiang, *Anal. Chem.* **2010**, *82*, 3002–6.

[11] C.-H. Wang, K.-Y. Lien, T.-Y. Wang, T.-Y. Chen, G.-B. Lee, *Biosens. Bioelectron.* **2011**, *26*, 2045–52.

[12] C.-H. Wang, K.-Y. Lien, J.-J. Wu, G.-B. Lee, *Lab Chip* **2011**, *11*, 1521–31.

[13] T. Konry, I. Smolina, J. M. Yarmush, D. Irimia, M. L. Yarmush, *Small* **2011**, *7*, 395–400.

[14] K. Sato, A. Tachihara, B. Renberg, K. Mawatari, K. Sato, Y. Tanaka, J. Jarvius, M. Nilsson, T. Kitamori, *Lab Chip* **2010**, *10*, 1262–6.

[15] I. K. Dimov, J. L. Garcia-Cordero, J. O'Grady, C. R. Poulsen, C. Viguier, L. Kent, P. Daly, B. Lincoln, M. Maher, R. O'Kennedy, et al., *Lab Chip* **2008**, *8*, 2071–8.

[16] A. Gulliksen, L. Solli, F. Karlsen, H. Rogne, E. Hovig, T. Nordstrøm, R. Sirevåg, *Anal. Chem.* **2004**, *76*, 9–14.

[17] A. Gulliksen, L. A. Solli, K. S. Drese, O. Sörensen, F. Karlsen, H. Rogne, E. Hovig, R. Sirevåg, *Lab Chip* **2005**, *5*, 416–20.

[18] M.-N. Tsaloglou, M. M. Bahi, E. M. Waugh, H. Morgan, M. Mowlem, *Anal. Methods* **2011**, *3*, 2127.

[19] J. Compton, *Nature* **1991**, *350*, 91–92.

[20] B. Graβ, A. Neyer, M. Jöhnck, D. Siepe, F. Eisenbeiβ, G. Weber, R. Hergenröder, *Sensors Actuators B* **2001**, *72*, 249–258.

[21] M. Castaño-Alvarez, M. T. Fernández-Abedul, A. Costa-García, *Anal. Bioanal. Chem.* **2005**, *382*, 303–10.

[22] C. S. Effenhauser, G. J. Bruin, A. Paulus, M. Ehrat, *Anal. Chem.* **1997**, *69*, 3451–7.

[23] L. Martynova, L. E. Locascio, M. Gaitan, G. W. Kramer, R. G. Christensen, W. A. MacCrehan, *Anal. Chem.* **1997**, *69*, 4783–9.

[24] R. M. McCormick, R. J. Nelson, M. G. Alonso-Amigo, D. J. Benvegnu, H. H. Hooper, *Anal. Chem.* **1997**, *69*, 2626–30.

[25] S. R. Nugen, P. J. Asiello, A. J. Baeumner, *Microsyst. Technol.* **2008**, *15*, 477–483.

[26] S. Qi, X. Liu, S. Ford, J. Barrows, G. Thomas, K. Kelly, A. McCandless, K. Lian, J. Goettert, S. A. Soper, *Lab Chip* **2002**, *2*, 88–95.

[27] M. A. Roberts, J. S. Rossier, P. Bercier, H. Girault, *Anal. Chem.* **1997**, *69*, 2035–42.

[28] X. Huang, W. J. Brittain, *Macromolecules* **2001**, *34*, 3255–3260.

[29] A. Bhattacharyya, C. M. Klapperich, *Anal. Chem.* **2006**, *78*, 788–92.

[30] N. C. Cady, S. Stelick, C. A. Batt, *Biosens. Bioelectron.* **2003**, *19*, 59–66.

[31] K. A. Hagan, J. M. Bienvenue, C. A. Moskaluk, J. P. Landers, *Anal. Chem.* **2008**, *80*, 8453–60.

[32] C. Liu, K. Lien, C. Weng, *Biomed. Microdevices* **2009**, *11*, 339–350.

[33] S. M. Berry, E. T. Alarid, D. J. Beebe, *Lab Chip* **2011**, *11*, 1747–53.

[34] M. S. Abrahamsen, T. J. Templeton, S. Enomoto, J. E. Abrahante, G. Zhu, C. A. Lancto, M. Deng, C. Liu, G. Widmer, S. Tzipori, et al., *Science* **2004**, *304*, 441–5.

[35] J. T. Connelly, S. R. Nugen, W. Borejsza-Wysocki, R. A. Durst, R. A. Montagna, A. J. Baeumner, *Anal. Bioanal. Chem.* **2008**, *391*, 487–95.

[36] Z. Bukhari, H. V. Smith, *Epidemiol. Infect.* **1997**, *119*, 105–108.

[37] S. R. Nugen, P. J. Asiello, J. T. Connelly, A. J. Baeumner, *Biosens. Bioelectron.* **2009**, *24*, 2428–33.

[38] C. W. Tsao, L. Hromada, J. Liu, P. Kumar, D. L. DeVoe, *Lab Chip* **2007**, *7*, 499–505.

[39] R. Benters, C. M. Niemeyer, D. Drutschmann, D. Blohm, D. Wöhrle, *Nucleic Acids Res.* **2002**, *30*, E10.

[40] E. T. Kang, K. L. Tan, K. Kato, Y. Uyama, Y. Ikada, *Macromolecules* **1996**, *29*, 6872–6879.

[41] E. Uchida, Y. Uyama, Y. Ikada, *Langmuir* **1993**, *9*, 1121–1124.

[42] A. J. Baeumner, M. C. Humiston, R. A. Montagna, R. A. Durst, *Anal. Chem.* **2001**, *73*, 1176–80.

[43] K. A. Edwards, A. J. Baeumner, *Anal. Bioanal. Chem.* **2006**, *386*, 1335–43.

[44] J. Min, A. J. Baeumner, *Anal. Biochem.* **2002**, *303*, 186–93.

[45] K. A. Edwards, A. J. Baeumner in *Biosensors and Biodetection* (Eds.: A. Rasooly, K. E. Herold), Humana Press/Springer, New York, **2009**, pp. 185-215.

[46] A. J. Baeumner, N. A. Schlesinger, N. S. Slutzki, J. Romano, E. M. Lee, R. A. Montagna, *Anal. Chem.* **2002**, *74*, 1442–8.

[47] Q. Ramadan, M. A. M. Gijs, *Microfluid. Nanofluidics* **2012**, *13*, 529–542.

[48] V. N. Goral, N. V Zaytseva, A. J. Baeumner, *Lab Chip* **2006**, *6*, 414–21.

CHAPTER 3

DEVELOPING NEW MATERIALS FOR PAPER-BASED DIAGNOSTICS USING ELECTROSPUN NANOFIBERS[2]

Abstract

The use of electrospun nanofibers as functional material in paper-based lateral flow assays (LFAs) was studied. Specific chemical features of the nanofibers were achieved by doping the base polymer, poly(lactic acid) (PLA), with poly(ethylene glycol) (PEG) and polystyrene$_{8K}$-*block*-poly(ethylene-*ran*-butylene)$_{25K}$-*block*-polyisoprene$_{10K}$-Brij76 (K3-Brij76) (KB). The LFAs were assembled such that the sample flowed through the nanofiber mat via capillary action. Initial investigations focused on the sustainable spinning and assembly of different polymer structures to allow the LFA format. Here, it was found that the base polymer poly(vinyl alcohol) (PVA), which had shown to function well in microfluidic biosensors, did not work in the LFA format. In contrast, PLA-based nanofibers enabled easy assembly. Three relevant features were chosen to study nanofiber-based functionalities in the LFA format: adsorption of antibodies, quantification of results, and non-specific binding. In particular, streptavidin-conjugated sulforhodamine B (SRB)-encapsulating liposomes were captured by anti-streptavidin antibodies adsorbed on the nanofibers. Varying the functional polymer concentration within the PLA base enabled the creation of distinct capture zones. Also, a sandwich assay for the detection of *Escherichia coli* (*E. coli*) O157:H7 was developed using anti-*E. coli* antibodies as capture and reporter species with horseradish peroxidase for signal generation. A dose-response curve for *E. coli* with a detection limit of 1.9×10^4 cells was

[2] This section has been reproduced with permission from Springer: S. J. Reinholt, A. Sonnenfeldt, A. Naik, M. W. Frey, A. J. Baeumner, *Anal. Bioanal. Chem.* **2013**, DOI 10.1007/s00216-013-7372-5 with modifications to conform to the required format.

achieved. Finally, functional polymers were used to demonstrate that non-specific binding can be eliminated using anti-fouling block copolymers. The enhancement of paper-based devices using functionalized nanofibers provides the opportunity to develop a broad spectrum of sensitive and specific bioassays with significant advantages over their traditional counterparts.

1 Introduction

The emerging field of paper-based microfluidic technology continues to gain great interest for the development of point-of-care assays. The complexity of these devices varies widely from basic dipsticks and lateral flow assays (LFAs) that have existed since the 1950s[1] to complex two- and three-dimensional microfluidic paper analytical devices (μPADs) recently pioneered by the Whitesides group.[2-6] There are many advantages to using a paper-based platform for producing point-of-care devices for use in resource-limited settings. Fabricating these devices out of paper makes them inexpensive, small, portable, and easily disposable.[2,4] These devices are also very easy to use and require no external equipment or power source due to their capillary wicking capability.[2,4]

There are a variety of materials used to construct these paper-based networks, and the type of paper selected depends on the specific characteristics required for device fabrication and operation. The paper materials used most commonly are cellulose fiber-based, which are biocompatible and can be chemically modified.[4,7,8] Laboratory filter and chromatography papers, such as those manufactured by Whatman, are often chosen as they are made from pure cellulose, are free of contaminants, and have a uniform pore size and thickness for uniform wicking.[4,8,9] Other papers used for these devices include hydrophobic and hydrophilic nitrocellulose, glossy

paper, and cellulose fiber matrices with a variety of different chemical modifications to alter their properties.[7-9]

Generally, the most important properties of the paper when fabricating paper-based devices for biological assays are pore size/wicking speed, surface area-to-volume ratio, and its chemical nature leading to functionalization, non-specific reactions and modifications for wicking speeds. An interesting and novel material in which these properties are all theoretically controllable is a mat made of electrospun nanofibers.[10-12]

Electrospinning is a process in which nanoscale fibers are produced using electrostatic forces generated between a charged polymer spinning solution and a grounded collector plate. The spinning solution is fed through a needle at a constant rate and a high voltage is applied between the needle and collector plate. This causes a Taylor cone to form at the tip of the needle. When a certain threshold voltage is reached, the electrostatic forces become greater than the surface tension, and a thin fiber is accelerated toward the collector plate forming an unwoven nanofiber mat. This process produces fibers with diameters between a few nanometers and a few micrometers.[12] The properties of the nanofiber mats can be controlled by changing the electrospinning parameters. Pore size and surface area-to-volume ratio scale with the diameter of the nanofibers.[10] The diameter of the nanofibers can be adjusted by altering the feed rate and polymer concentration of the spinning solution,[10-12] and to a lesser extent the applied voltage and distance between the needle and collector plate.[10] The chemical characteristics of the nanofiber surface can be changed by using different types of polymers and combinations of polymers in different ratios. Cho *et al.* created positive and negative nanofibers by electrospinning poly(vinyl alcohol) (PVA) nanofibers with hexadimethrine bromide (Polybrene) and poly(methyl vinyl ether-alt-maleic anhydride) (poly(MVE/MA)), respectively.[13] Tamura and Kawakami produced

electrospun nanofibers that had both hydrophobic and hydrophilic domains within the same nanofiber by using the block copolymer, NTDA-BDSA-r-APP.[14] The properties of the nanofiber mat can thus be catered to the specific application in which it will be used.

In this study, we investigate the use of poly(lactic acid) (PLA)-based electrospun nanofibers in an LFA format to determine the feasibility of incorporating nanofibers into paper-based devices and using nanofibers as a platform for paper-based biological assays. The surface properties of the PLA nanofibers were adjusted by adding additional polymers to the spinning solution: poly(ethylene glycol) (PEG) to increase the hydrophilicity and polystyrene$_{8K}$-*block*-poly(ethylene-*ran*-butylene)$_{25K}$-*block*-polyisoprene$_{10K}$-Brij76 (K3-Brij76) (KB) to eliminate non-specific binding of biological species. Immobilization of antibodies through simple adsorption to the nanofibers was also demonstrated and utilized to develop biological assays in an LFA format.

2 Methods

2.1 Electrospinning

PLA nanofiber mats were electrospun as previously described.[15] In our experiments, a different gauge of needle was used and the collector plate was at a different distance from the spinning needle tip. Briefly, a spinning solution of 22wt% PLA (Jamplast 4043D) in dimethylformamide (DMF) (Sigma Aldrich) was prepared at 70°C using a heated stir plate (VWR) for 90 minutes. The spinning solution was loaded into a 5mL glass syringe (Cadence Science), and a 20-gauge deflected-point needle (Cadence Science) was used. The solution was pumped from the syringe at a rate of 10µL/min using a programmable syringe pump (Harvard Apparatus). The syringe and needle were heated to 70°C during the spinning process using a heating element and VariTemp Blower, respectively. A 15kV voltage was applied to the needle relative to the 4x4cm

grounded collector plate positioned 10cm from the tip of the needle, and the nanofibers were spun for 30 minutes. To produce PLA-PEG nanofibers, 3wt% PEG was added to the 22wt% PLA spinning dope, and the same spinning conditions were applied.

The triblock terpolymer, polystyrene$_{8K}$-*block*-poly(ethylene-*ran*-butylene)$_{25K}$-*block*-polyisoprene$_{10K}$-Brij76 (K3-Brij76) (KB), is an amphiphilic polymer that was previously synthesized to produce nanofibers with anti-fouling properties.[16] A polymer spinning dope solution of 40/60wt% PLA (Jamplast 6201D)/KB in 3:1 v/v chloroform/acetone (Sigma Aldrich) was used to synthesize these nanofibers. The nanofibers were spun using a flow rate of 0.03mL/min and a voltage of 17kV.

2.2 Assembly of LFAs and Signal Recording

A simple setup was used to assemble the LFAs incorporating nanofibers. A nanofiber mat (4.5x150mm or 1.75x5mm) was adhered directly to a backing card (Millenia Diagnostics) 4.5mm in width, so the nanofiber mat remained fixed during sample flow. The backing cards are sheets of polyvinyl chloride (PVC) plastic with an adhesive layer, so the sample will not flow into the backing cards. An absorbent pad (Millipore) 10x120mm was placed on the backing card such that it overlapped with the nanofiber mat by approximately 2mm. The absorbent pad facilitates capillary flow of the sample through the nanofiber matrix. Figure 3.1 shows a schematic of the simple LFA setup, as well as a schematic of the sandwich binding assay. The assembly of each LFA took approximately 1 minute. For each assay described, the signal was colorimetric. An image of the LFAs was taken, and the image was analyzed using ImageJ software to quantify the color intensity. These intensities were always compared to several negative controls.

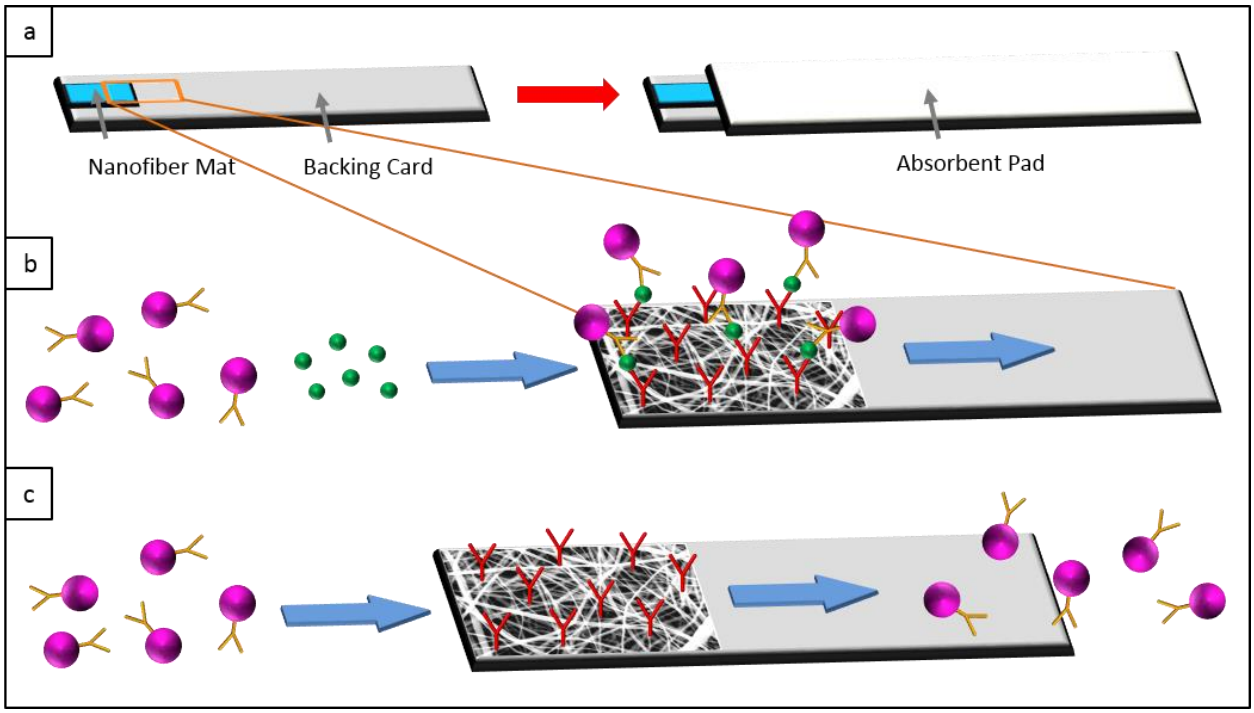

Figure 3.1: Schematic of LFA format and sandwich binding assay. A 1.75x5mm nanofiber mat was placed directly on a backing card 4.5mm in width, and a 1x20cm absorbent pad was placed on the backing card overlapping the nanofiber mat by approximately 2mm (a). The LFAs ran vertically in glass culture tubes. In the E. coli sandwich assay, E. coli (green) flowed through the anti-E. coli-modified nanofiber mat, followed by horseradish peroxidase (HRP)-conjugated (pink) anti-E. coli. When E. coli is present, a colorimetric signal results upon addition of HRP substrate (b), and when no E. coli is present, the HRP antibodies flow through the nanofiber mat and no signal is observed (c).

2.3 Single-Step Binding Assay

PLA and PLA-PEG nanofiber mats were used in the LFA configuration described above to facilitate a single-step binding assay. In this colorimetric assay, anti-streptavidin antibodies (VWR SP-4000) were used to capture streptavidin-conjugated sulforhodamine B (SRB)-encapsulating liposomes, which were synthesized as previously described by our group.[17] The nanofiber mats were prewet with a solution of 5% methanol in 1x 2-Amino-2-hydroxymethyl-propane-1,3-diol (Tris)-Buffered Saline (1xTBS) to increase the hydrophilicity of the nanofibers allowing solutions to wick through the mat more efficiently via capillary action. The nanofibers were submerged in this solution for approximately 10 minutes, and then the nanofiber mats were

placed in a vacuum oven to dry for 60 minutes at 40°C and 15 in. Hg. The nanofiber mats were cut to 4.5x150mm and adhered to the backing card as described above. A 500µg/mL anti-streptavidin antibody solution in 0.4M $NaHCO_3/Na_2CO_3$ pH 9 was prepared, and 1µL of this solution was pipetted onto each nanofiber mat. The samples were dried in a vacuum oven for 90 minutes at 40°C and 15 in. Hg. The nanofiber mats were then blocked with a solution of 0.1% polysorbate 20 (Tween-20), 0.1% Na-casein, and 0.25% sucrose for 5 minutes. The samples were subsequently dried in a vacuum oven overnight at room temperature and 15 in. Hg.

A 1mM solution of streptavidin-conjugated SRB-encapsulating liposomes in 1x 2-[4-(2-hydroxyethyl)piperazin-1-yl]ethanesulfonic acid (HEPES)-sucrose-saline (1xHSS) was prepared. A 3µL volume of liposome solution was pipetted into 12x75mm glass culture tubes (VWR), and the nanofiber LFAs were placed vertically into the culture tubes such that the end of the nanofiber mat was in contact with the liposome solution and the solution wicked up. Unbound liposomes were washed away in the same fashion using 60µL of 1xHSS in a fresh culture tube. A nitrocellulose control was performed in the same manner as the nanofiber assays. Negative controls contained no anti-streptavidin antibodies. Another negative control for the PLA-PEG nanofibers was to use liposomes without streptavidin on their surface to determine whether any non-specific binding to the antibody-coated nanofibers occurred.

2.4 E. coli Sandwich Assay

To prepare an *Escherichia coli* (*E. coli*) O157:H7 liquid culture, a 2wt% aqueous solution of LB broth (Fisher Scientific) was prepared and autoclaved, and 5mL was added to a culture tube. This solution was inoculated with *E. coli* O157:H7 and placed in a shaking incubator at 37°C and 220 rpm for 24 hours.

PLA-PEG nanofibers were used for this assay. The nanofibers were prewet as before with a 5% methanol solution in 1xTBS, and dried in a vacuum oven at 40°C and 15 in. Hg for 60 minutes. The nanofibers were cut into 1.75x5 mm mats and the LFAs were assembled as described above. A 1mg/mL anti-*E. coli* capture antibody (Abcam ab20976) solution in 0.4M $NaHCO_3/Na_2CO_3$ pH 9 was prepared, and 0.5µL of this solution was pipetted onto each nanofiber mat. The samples were dried in a vacuum oven for 90 minutes at 40°C and 15 in. Hg. The nanofiber mats were then blocked with a solution of 2% bovine serum albumin (BSA), 0.1% polysorbate 20 (Tween-20), 0.1% Na-casein, and 0.25% sucrose for 30 minutes. Next, the samples were dried in a vacuum oven overnight at room temperature and 15 in. Hg.

The concentration of the liquid *E. coli* culture was determined by measuring the optical density at a 600nm wavelength, and the *E. coli* was diluted to the desired concentration in LB broth. A volume of 5µL of *E. coli* solution was pipetted into glass culture tubes, and the LFAs were placed into the culture tubes vertically, so only the edge of the nanofiber mat was in contact with the solution. The solution was allowed to wick up completely, and then the nanofibers were washed in the same vertical fashion using 60µL of 1xHSS in a new culture tube. A 500µg/mL solution of horseradish peroxidase (HRP)-conjugated anti-*E. coli* reporter antibodies (Abcam ab20425) in 1x phosphate-buffered saline (1xPBS) was prepared and 1µL of this solution was pipetted onto the bottom edge of the nanofiber mat and allowed to flow through the mat horizontally. Excess reporter antibody was washed out of the nanofiber mat vertically using 240µL of 1xHSS. After washing, the absorbent pad was removed from the LFA to prevent flow, and 7µL of the HRP substrate, 1-Step 2,2'-Azinobis [3-ethylbenzothiazoline-6-sulfonic acid]-diammonium salt (ABTS) (Thermo Scientific), was pipetted onto the whole nanofiber mat. The colorimetric substrate reaction was allowed to continue for 10 minutes, and a blue-green color resulted. Two

types of negative controls were used in this assay. The first omitted both the capture antibody and the *E. coli* cells to test the efficacy of the final wash step. The second negative control was an LFA without capture antibody that tested how well the unbound *E. coli* cells washed out of the nanofibers. A schematic representation of this assay is shown in Figure 3.1b and 3.1c.

2.5 Nanofibers for Eliminating Non-Specific Binding

The PLA-KB nanofiber mats were prewet for 10 minutes with a solution of 5% methanol in 1xTBS, and dried in a vacuum oven for 60 minutes at 40°C and 15 in. Hg. The nanofibers were cut into 1.75x5mm mats and assembled into the LFA format described above. A 1mM solution of carboxylated SRB-encapsulating liposomes was prepared, and 5µL were allowed to wick up the nanofiber mat vertically within a glass culture tube. The unbound liposomes were then washed out of the nanofiber mat vertically using 60µL of 1xHSS. The nanofiber mats were imaged with a fluorescence microscope to observe any non-specific liposome binding that occurred. These nanofibers were compared to PLA nanofibers that had been prewet, were either blocked or unblocked, and underwent the same testing process.

3 Results and Discussion

Previously, our lab demonstrated that PVA-polybrene nanofibers within a microfluidic channel can capture carboxylated SRB-encapsulating liposomes electrostatically, and release them upon an increase in pH.[18] The attempt to incorporate this attractive feature into a paper-based assay; however, was unsuccessful as the mechanical properties of the nanofibers were unfavorable for assembly in an LFA format for both external manipulations and wicking actions. While thicker mats overcame some of these challenges, the resulting denser mat made fluid flow difficult. In contrast, PLA functioned very well as the nanofiber base polymer. An important characteristic of

LFA material is the achievable wicking rate as it directly influences contact time between biological assay components. The wicking rate of the nanofibers can be adjusted by changing the pore size of the spun mat. In the experiments described below, the wicking rates varied slightly due to minimal differences in thicknesses and pore sizes. These differences were caused by varying atmospheric conditions during spinning. More reproducible nanofiber mats could be spun given a temperature- and humidity-controlled chamber. Nonetheless, highly reproducible wicking rates and functionalities were obtained when comparing different nanofiber mats. During an assay, the wicking rate changed as the solution wicked into the absorbent pad. The wicking rate slowly decreased as the absorbent pad became increasingly saturated, which occurs in any LFA based on porous material. The wicking rate on average was 5uL/min.

3.1 Single-Step Binding Assay

The ability to incorporate electrospun nanofibers successfully into an LFA was assessed using a simple single-step binding assay. Initially, 22wt% PLA nanofibers were spun and the mat was used in an assay that involved immobilizing anti-streptavidin antibodies via adsorption onto the nanofiber mat and capturing the streptavidin-conjugated SRB-encapsulating liposomes that flowed through the mat. Figure 3.2a and 3.2b show scanning electron microscopy (SEM) images of the 22wt% PLA nanofibers at two different magnifications. The quality of the assay results was promising (see further below). As PLA mats were hydrophobic, varying concentrations of PEG were added to the spinning solution, and a final concentration of 3wt% PEG was chosen for the 22wt% PLA nanofibers. Figure 3.2c shows an SEM image of the 22wt%/3wt% PLA/PEG nanofibers. Figure 3.2d shows a fluorescent confocal microscopy image of the PLA-PEG nanofibers where the green color represents the natural fluorescence of PEG. Since PEG is

hydrophilic, it phase separates preferentially to the outer surface of the PLA nanofibers as was also shown by Hendrick and Frey.[19]

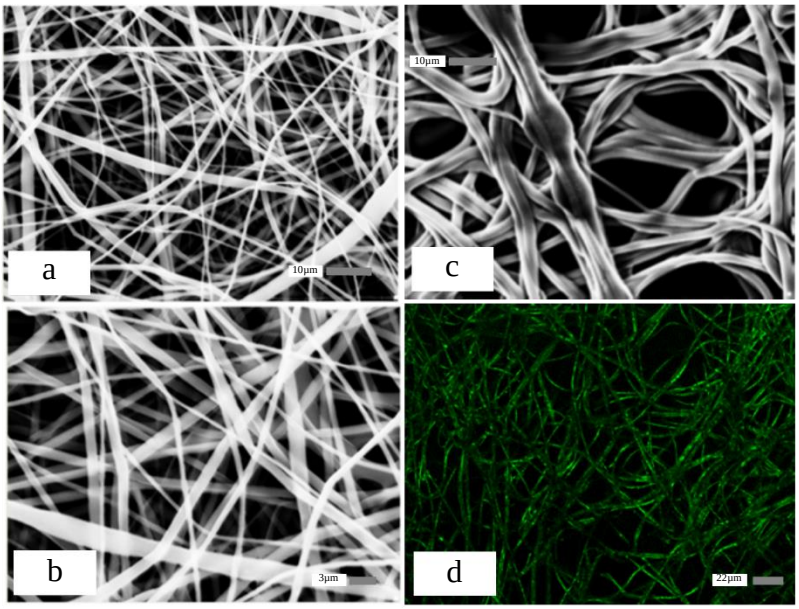

Figure 3.2: Microscopic Images of PLA and PLA-PEG Nanofibers. SEM images of 22wt% PLA nanofibers at different magnifications (a and b) and an SEM image of 22wt% PLA-3%wt% PEG (c) were taken. A confocal microscope image of 22wt% PLA-3%wt% PEG is shown in where the natural fluorescence of PEG shows that the PEG is on the periphery of the nanofibers (d).

After assembly of the nanofiber LFAs, 1µL of the 500µg/mL anti-streptavidin antibody solution was pipetted onto the nanofiber mats. The size and shape of the capture area containing the immobilized antibodies was dependent on the hydrophobicity and thickness of the nanofiber mat. The PLA nanofibers produced the widest dispersion of the antibodies and the adsorption area was irregularly shaped. This is potentially due the hydrophobicity of the nanofibers as the droplet of antibody solution wicked across the surface of the nanofiber mat as opposed to penetrating down into the mat, and the irregular shape was the solution wicking through the paths of least resistance. The PLA-PEG nanofibers showed less dispersion of the antibody droplet, but still gave an irregular shape. In this case the solution wicked down into the full thickness of the nanofiber mat; however, there was still excess solution that wicked along the length of the nanofiber mat following paths

of least resistance. To improve the shape of the capture zone, and therefore the appearance of the results, a thicker PLA-PEG nanofiber mat was electrospun and tested. A thicker mat decreased the amount of spreading observed and a circular capture zone was achieved. Images of the different nanofiber mats are inset in Figure 3.3 where PLA-PEG 1 is a thinner mat compared to PLA-PEG 2. Nitrocellulose controls were performed and circular capture zones were also achieved in this case, although the PLA-PEG was better at producing sharper edges.

A volume of 3µL of 1mM streptavidin-conjugated SRB-encapsulating liposomes were allowed to flow through the LFAs after the antibodies were immobilized, and the unbound liposomes were washed out using 60µL of 1xHSS. The colorimetric results were quantified using ImageJ software. The results for the different nanofiber mats as well as the nitrocellulose control are displayed in Figure 3.3. The results show that on average, the thicker PLA-PEG nanofiber mat elicits a more intense signal than the PLA and thinner PLA-PEG nanofibers. It should also be noted that the signal is comparable to the nitrocellulose control. In all cases, non-specific binding as shown by the negative controls, was negligible, with the PLA-PEG mat again outperforming the plain PLA mat. Also, here, the PLA-PEG mats performed comparably with the nitrocellulose membranes, which is an important initial characteristic needed to then add further capabilities into the nanofiber mats that cannot be achieved in standard nitrocellulose designs. Similarly, non-specific binding of liposomes (without streptavidin), which can occur in nitrocellulose settings,[20] was shown to be negligible for the PLA-PEG mats ("C" in Figure 3.3). With the single-step assay successfully demonstrated and an appropriate nanofiber mat selected, a sandwich assay using a bacteria of interest, pathogenic *E. coli* O157:H7, was developed using a different signal amplification system to further study the general applicability of nanofiber mats in an LFA format.

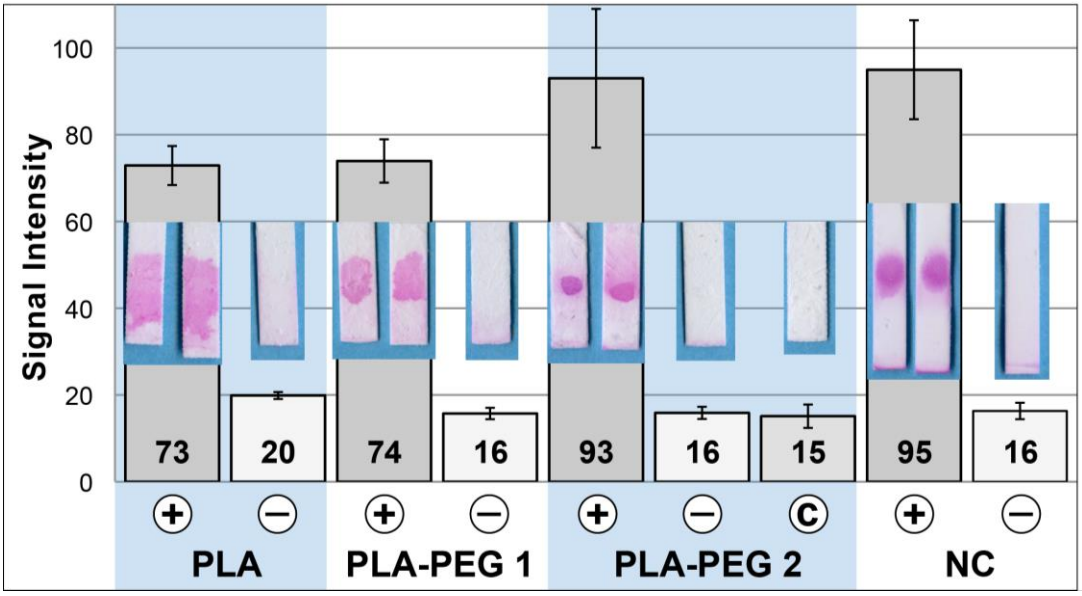

Figure 3.3: Signal comparison of the anti-streptavidin antibody/streptavidin-conjugated liposome LFA using PLA nanofibers, PLA-PEG nanofibers, and nitrocellulose (NC). Anti-streptavidin antibodies were immobilized on the positive LFAs, but not the negative LFAs. The "C" indicates a negative control that used C. parvum reporter probe liposomes instead of streptavidin liposomes to test for non-specific liposome binding. PLA-PEG 2 samples were LFAs with thicker nanofiber mats than PLA-PEG 1. The signal was analyzed using ImageJ software.

3.2 E. coli Sandwich Assay

Using the optimal PLA-PEG nanofiber mat, a sandwich assay for *E. coli* O157:H7 was developed similarly to the single-step binding assay. Two antibodies specific to *E. coli* O157:H7 were used. The capture antibody was immobilized onto the nanofiber mat, and the reporter antibody was conjugated with HRP. The signal was produced by adding a substrate for HRP, 1-Step ABTS, that undergoes a color change to display a colorimetric result. Several different *E. coli* concentrations ranging from $5x10^3$ to $7.5x10^5$ cells/LFA were tested, and the colorimetric results were quantified using ImageJ software. A thorough dose-response curve, shown in Figure 3.4, was generated and the limit of detection was determined to be $1.9x10^4$ cells. This limit of detection is comparable to other published immunoassays for bacteria.[21-25] The relevant negative controls in

these experiments tested for non-specific binding of both the *E. coli* cells and also the HRP-conjugated reporter antibodies. The signal from non-specific binding of the reporter antibodies is represented as the zero concentration in the dose-response curve in Figure 3.4, and is negligible. Non-specific retention of *E. coli* in the nanofiber mats was tested at every *E. coli* concentration by omitting the capture antibody immobilization step. These results showed similar levels of signal as the zero-concentration samples, so importantly, the *E. coli* cells are not bound non-specifically to the PLA-PEG nanofiber mats. These results demonstrate that a successful sandwich immunoassay in an LFA format is possible using a platform of electrospun nanofibers.

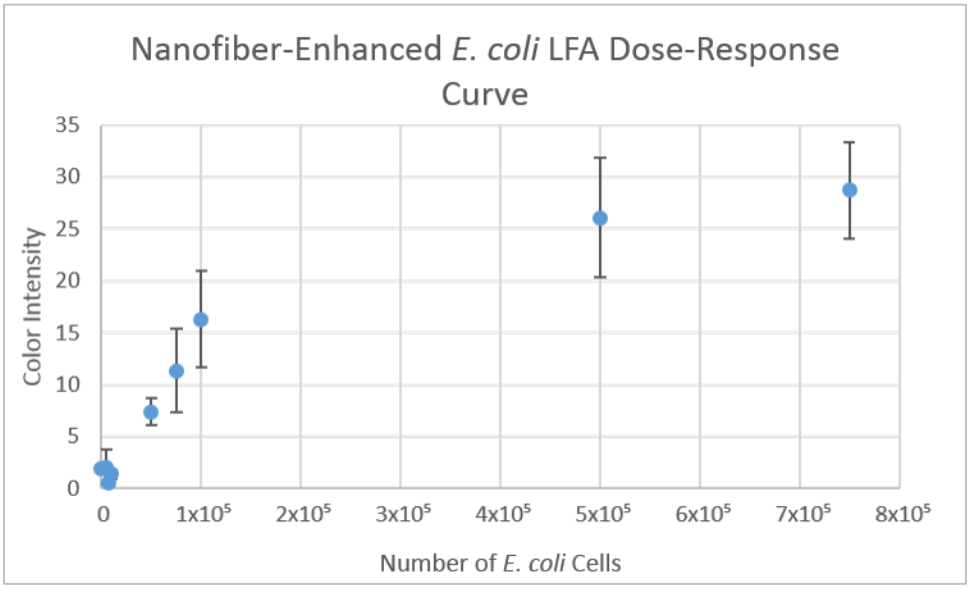

Figure 3.4: Nanofiber-Enhanced E. coli LFA Signal Dose-Response Curve. Anti-E. coli antibodies were immobilized on PLA-PEG nanofibers. A sandwich assay was performed in which E. coli bound to the capture antibody, and a reporter antibody conjugated with HRP bound to the captured E. coli cells to produce a colorimetric signal when substrate was added. The signal was analyzed using ImageJ. The limit of detection was calculated to be 1.9×10^4 cells.

3.3 Nanofibers for Eliminating Non-Specific Binding

The previously described thorough studies with respect to negative controls indicate the importance non-specific binding has especially in simple field and on-site assays. Even though

PEG is often times included in biological assays to avoid non-specific binding,[26] its presence in the PLA-PEG nanofibers was not sufficient for this purpose. We therefore investigated further approaches to eliminate non-specific binding not only via blocking reactions, but also more attractively via direct incorporation of anti-fouling polymers. Thus, an additional polymer, KB, was added to the PLA nanofibers. PLA-KB nanofibers completely eliminated the non-specific binding of the carboxylated SRB-encapsulating liposomes without the use of blocking agents likely due to repulsive forces between the nanofibers and liposomes. These nanofibers were compared to the non-specific binding of liposomes to unblocked and blocked PLA nanofibers. Figure 3.5a shows fluorescence images of unblocked and blocked PLA and unblocked PLA-KB nanofibers after they have been exposed to liposomes and washed. The PLA nanofibers had a very high level of non-specific binding, while the PLA-KB nanofibers had no visible non-specific interactions with the liposomes. The level of non-specific binding was quantified using ImageJ software, and Figure 3.5b shows the results of this analysis. The complete elimination of non-specific binding makes these nanofibers an extremely attractive material for developing highly sensitive paper-based biological assays.

4 Conclusions

Paper-based platforms have become increasingly popular for developing point-of-care assays, as they are inexpensive, portable, disposable, easy to use, and require no external equipment. In this study, we have presented PLA-based electrospun nanofibers as a new material and alternative to the standard cellulose-based papers for use in paper-based assays such as LFAs. PLA-PEG nanofibers were synthesized and incorporated into an LFA, and a single-step binding assay using anti-streptavidin antibodies and streptavidin-conjugated SRB-encapsulating liposomes

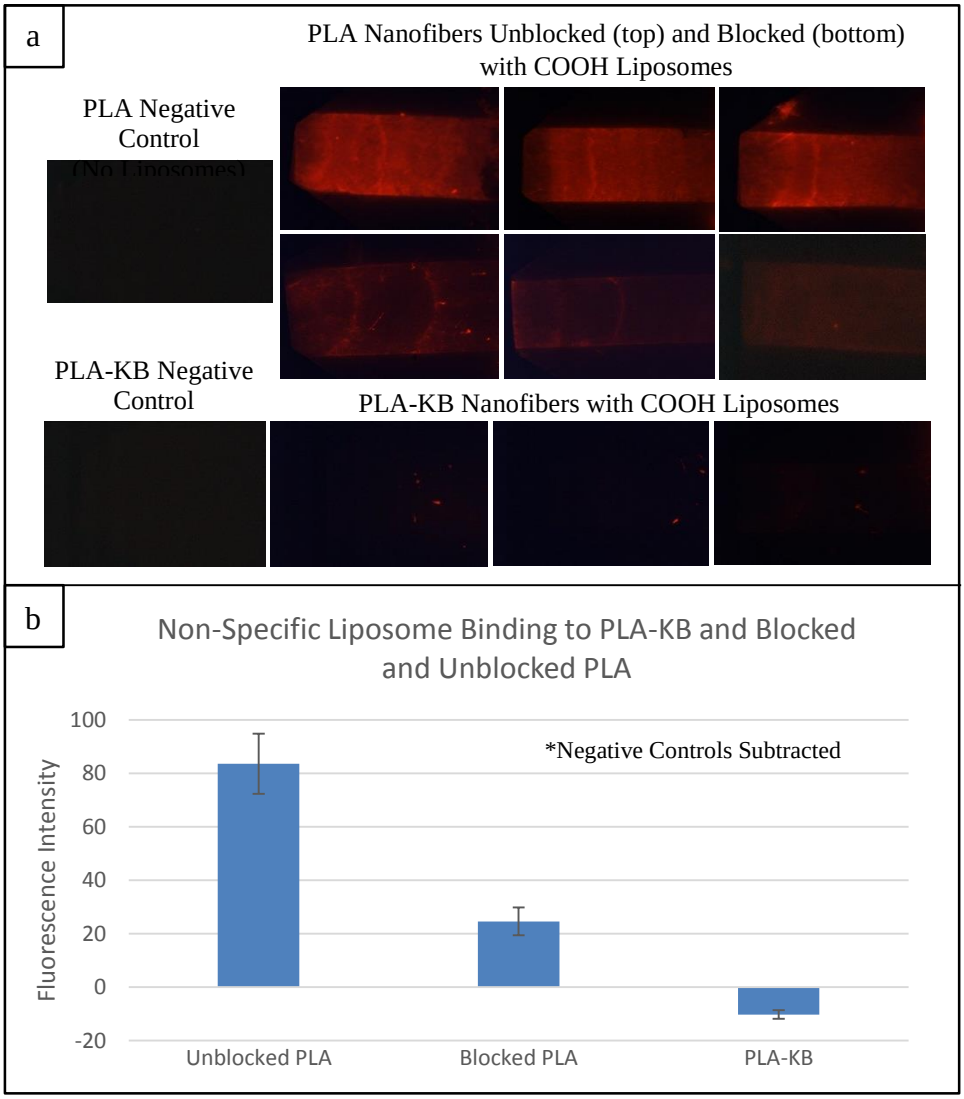

Figure 3.5: Comparison of Non-Specific Liposome Binding to PLA-KB and Blocked and Unblocked PLA Nanofibers. 20µL of 100µM carboxylated liposomes wicked through PLA-KB nanofibers and PLA nanofibers, and the nanofibers were washed with 60µL of 1xHSS. Fluorescence images of nanofibers after testing (a), and a quantitative measurement of the non-specific liposome binding (b) are shown.

was developed. The properties of the nanofiber mat and the conditions of the assay were optimized to achieve a result that was comparable to the nitrocellulose control. These nanofibers were then used to develop an enzymatic sandwich immunoassay for *E. coli* O157:H7 in the same LFA format. A dose-response curve for this assay determined the limit of detection to be 1.9×10^4 cells. Furthermore, an amphiphilic triblock terpolymer, KB, was incorporated into the PLA nanofibers and produced nanofibers with the ability to completely eliminate non-specific binding of

carboxylated SRB-encapsulating liposomes without the use of any blocking reagents. This attractive characteristic will be further investigated in the future with respect to its impact on the optimization of binding assay performances in the LFA format. These results not only demonstrate the general applicability of electrospun nanofiber mats in LFA formats, but provide insight into the immense possibilities offered by this new avenue of research. Novel materials will provide many opportunities for paper-based diagnostic development. Specific surface chemistries can be tailored to specific analytical challenges, notorious non-specific binding, especially obtained in complex matrices, can be overcome by smart material design. Here, investigations for covalent bonding of antibodies to the nanofibers will be required to fully explore their capabilities. Electrospun nanofibers will therefore have a significant impact on the field of paper-based microfluidic analytical devices with their desirable properties that are entirely controllable.

5 References

[1] A. H. Free, E. C. Adams, M. L. Kercher, H. M. Free, M. H. Cook, *Clin. Chem.* **1957**, *3*, 163–8.

[2] A. W. Martinez, S. T. Phillips, M. J. Butte, G. M. Whitesides, *Angew. Chem. Int. Ed. Engl.* **2007**, *46*, 1318–20.

[3] A. W. Martinez, S. T. Phillips, B. J. Wiley, M. Gupta, G. M. Whitesides, *Lab Chip* **2008**, *8*, 2146–50.

[4] A. W. Martinez, S. T. Phillips, G. M. Whitesides, E. Carrilho, *Anal. Chem.* **2010**, *82*, 3–10.

[5] C.-M. Cheng, A. D. Mazzeo, J. Gong, A. W. Martinez, S. T. Phillips, N. Jain, G. M. Whitesides, *Lab Chip* **2010**, *10*, 3201–5.

[6] C.-M. Cheng, A. W. Martinez, J. Gong, C. R. Mace, S. T. Phillips, E. Carrilho, K. A. Mirica, G. M. Whitesides, *Angew. Chemie* **2010**, *122*, 4881–4884.

[7] R. Pelton, *TrAC Trends Anal. Chem.* **2009**, *28*, 925–942.

[8] D. D. Liana, B. Raguse, J. J. Gooding, E. Chow, *Sensors (Basel).* **2012**, *12*, 11505–26.

[9] E. W. Nery, L. T. Kubota, *Anal. Bioanal. Chem.* **2013**, DOI 10.1007/s00216-013-6911-4.

[10] D. Hussain, F. Loyal, A. Greiner, J. H. Wendorff, *Polymer* **2010**, *51*, 3989–3997.

[11] L. Huang, N.-N. Bui, S. S. Manickam, J. R. McCutcheon, *J. Polym. Sci. Part B Polym. Phys.* **2011**, *49*, 1734–1744.

[12] A. Baji, Y.-W. Mai, S.-C. Wong, M. Abtahi, P. Chen, *Compos. Sci. Technol.* **2010**, *70*, 703–718.

[13] D. Cho, L. Matlock-Colangelo, C. Xiang, P. J. Asiello, A. J. Baeumner, M. W. Frey, *Polymer* **2011**, *52*, 3413–3421.

[14] T. Tamura, H. Kawakami, *Nano Lett.* **2010**, *10*, 1324–8.

[15] D. Li, M. W. Frey, Y. L. Joo, *J. Memb. Sci.* **2006**, *286*, 104–114.

[16] Y. Cho, D. Cho, J. H. Park, M. W. Frey, C. K. Ober, Y. L. Joo, *Biomacromolecules* **2012**, *13*, 1606–14.

[17] K. A. Edwards, K. L. Curtis, J. L. Sailor, A. J. Baeumner, *Anal. Bioanal. Chem.* **2008**, *391*, 1689–702.

[18] L. Matlock-Colangelo, D. Cho, C. L. Pitner, M. W. Frey, A. J. Baeumner, *Lab Chip* **2012**, *12*, 1696–701.

[19] E. S. Hendrick, M. W. Frey, Increasing surface hydrophilicity in poly(lactic acid) electrospun fibers by addition of PLA-b-PEG co-polymers, *J. Eng. Fiber Fabr.* **2013**, accepted 4/26/2013 in press.

[20] M. Galli, P. Comfurius, C. Maassen, H. C. Hemker, M. H. de Baets, P. J. C. van Breda-Vriesman, T. Barbui, R. F. A. Zwaal, E. M. Bevers, *Lancet* **1990**, *335*, 1544–1547.

[21] S. Park, H. Kim, S.-H. Paek, J. W. Hong, Y.-K. Kim, *Ultramicroscopy* **2008**, *108*, 1348–51.

[22] K.-H. Seo, P. S. Holt, H. D. Stone, R. K. Gast, *Int. J. Food Microbiol.* **2003**, *87*, 139–144.

[23] A. H. Peruski, L. F. Peruski, *Clin. Vaccine Immunol.* **2003**, *10*, 506–513.

[24] S. Hearty, P. Leonard, J. Quinn, R. O'Kennedy, *J. Microbiol. Methods* **2006**, *66*, 294–312.

[25] T. Vollmer, D. Hinse, K. Kleesiek, J. Dreier, *J. Clin. Microbiol.* **2010**, *48*, 3475–81.

[26] P. T. Charles, V. R. Stubbs, C. M. Soto, B. D. Martin, B. J. White, C. R. Taitt, *Sensors* **2009**, *9*, 645–55.

CHAPTER 4

SUMMARY AND CONCLUSIONS

A key challenge in the miniaturization of nucleic acid detection techniques has been addressed in this research. Through the combination of an mRNA isolation and amplification step within the same location, a high sensitivity was achieved with the elimination of losses during sample transfer. Most important was the preparation of the microchannel surface to enable efficient isolation on one hand, and amplification without release of the mRNA from the surface on the other hand. We postulate that the effectiveness of the PAMAM dendrimer surface is not only due to the availability of more immobilization sites, but also due to an ideal surface in which the mRNA is not bound too tightly so as to prevent amplification or bound too loosely that it will be washed out of the channel. Furthermore, the surface chemistry presented an environment where there was no non-specific binding of the NASBA enzymes, which was a constant problem among previous devices.

Similar approaches to achieving high sensitivity through the exploitation of coupling isolation and amplification together within the same chamber, as well as amplifying the NAs without releasing them from the extraction media, have been reported previously. For example, Oblath *et al.* were able to detect as little as 300 fg of DNA using an aluminum oxide membrane on which the NAs remain immobilized during amplification.[1] Also, Zhang *et al.* achieved detection of a single bacterial cell using liquid-phase separation via phenol-chloroform extraction, followed by amplification within the same chamber.[2] When evaluating a device for NA isolation, it is important to determine how the NAs are being bound to the surface. One method for studying the bound NAs is through the use of fluorescence microscopy, which was used by Prinz *et al.* to determine where their target DNA resided in the microdevice.[3] Determining the yield of isolated

NAs from the initial sample is also necessary to assess the efficiency of the process, which is crucial for the detection of low concentrations of NAs. This can be measured using several methods. Many of the researchers that report low limits of detection use gel electrophoresis and a method for determining the approximate yield of NAs.[4-7] Fluorescent reporters can also be used[1, 8], as well as commercial quantitative assays such as the PicoGreen assay.[9] For highly accurate determinations of the NA yield from sample with very low target concentrations, quantitative PCR can also be used.[10]

A simpler type of biosensor using lateral flow assay technology was developed and enhanced using electrospun PLA-based nanofibers incorporating functional polymers, which provided beneficial properties to improve performance. Although comparison of the nanofiber LFAs with nitrocellulose showed fairly equivalent performance, nanofiber mats are not yet ready to compete with existing, well-established nitrocellulose technology. Nitrocellulose mats can be manufactured to be extremely uniform and possess the same properties from mat to mat. However, this is not true of the nanofiber mats described here. Due to the uncontrollable environmental conditions during the electrospinning process, the pore size and thickness of the nanofiber mats greatly varied between batches. This resulted in variations in flow rate and immobilization of the capture antibodies, which affected the quality and consistency of results. Additionally, the nanofibers required an extra pre-wetting process before the antibodies could be immobilized, which poses further variances to the flow rate and capture efficiency. Nanofiber mats are also more difficult to handle, which makes them less user-friendly.

Despite the challenges associated with using nanofibers in paper-based systems, the potential advantages are monumental, which makes them well worth studying further. First and foremost, nanofibers offer considerably higher surface area-to-volume ratios than other materials,

which greatly increases the number of available binding sites to immobilize biorecognition elements. This will have a significant impact on the sensitivity and efficiency of the device. The nanoscale dimensions of the nanofiber mats also allow for much faster mass transfer rates, which can lead to faster analysis and lower limits of detection. In addition, through simple adjustments of the electrospinning process, the characteristics of the nanofibers can be customized and easily tuned to the specific assay needs, which provides the opportunity to optimize the platform for highly sensitive detection. Furthermore, nanofibers can be spun from a very wide range of biocompatible materials with different properties. This enables countless functionalization options to facilitate the detection of limitless possible biological species.

To allow nanofibers to be easier to use within paper-based analytical devices, some aspect of their fabrication, handling, and use should be simplified. Control of the atmospheric conditions in the electrospinning chamber is paramount to producing consistent, high quality nanofiber mats. Eliminating the need to transfer the nanofiber mat from the collector plate material to the paper-based system is also beneficial not only in making the process more user-friendly, but also because it reduces contamination. This can be achieved by electrospinning the nanofibers directly on the assay backing material. The preparation of the nanofibers should also be simplified in that fewer steps should be required to perform the necessary modifications to facilitate the assay.

A unique approach to simplifying the nanofiber preparation is through the incorporation of additional materials in the electrospinning dope. This has the potential to produce nanofiber mats that are completely ready to facilitate the bioassay without any additional preparation, which is the ultimate goal and advantage to using electrospun nanofibers. With this method, the nanofibers must possess wettability, available biorecognition species on their surface, and the ability to

prevent non-specific interactions. These are the aspects of nanofiber technology that must be explored further to realize their full potential in bioanalytical devices.

Research presented here demonstrated the prevention of non-specific binding using functional anti-fouling polymers spun directly into the nanofibers. This technology should be studied further as non-specific binding is a current limitation of cellulose-based LFAs, and its elimination would result in lower detection limits for nanofiber-based assays. Incorporation of biological species, namely proteins, into the electrospinning dope itself has also been studied, but has yielded little success. The harsh conditions of the electrospinning process, including high heat and organic solvents, could be denaturing the proteins. Another possibility is that the proteins are being rendered unavailable due to their location within the nanofibers (not on the surface), or their orientation. Exploration into successful electrospinning of biorecognition elements into the nanofiber mats should be done as this would truly demonstrate the incredible potential of this technology.

Exploration of new techniques and materials is very important for developing novel biosensors that can overcome the limitations that restrict the use and efficacy of currently used technologies. Through the creation of innovative solutions to universal problems associated with existing μTAS designs, highly sensitive and specific biosensors can be realized for truly point-of-care applications.

1 References

[1] E. A. Oblath, W. H. Henley, J. P. Alarie, J. M. Ramsey, *Lab Chip* **2013**, 13, 1325–32.

[2] R. Zhang, H.-Q. Gong, X. Zeng, C. Lou, C. Sze, *Anal. Chem.* **2013**, *85*, 1484–91.

[3] C. Prinz, J. O. Tegenfeldt, R. H. Austin, E. C. Cox, J. C. Sturm, *Lab Chip* **2002**, *2*, 207–12.

[4] J. S. Marcus, W. F. Anderson, S. R. Quake, *Anal. Chem.* **2006**, *78*, 3084–9.

[5] D. Liu, G. Liang, Q. Zhang, B. Chen, *Anal. Chem.* **2013**, *85*, 4698–4704.

[6] C.-H. Wang, K.-Y. Lien, T.-Y. Wang, T.-Y. Chen, G.-B. Lee, *Biosens. Bioelectron.* **2011**, *26*, 2045–52.

[7] C.-H. Wang, K.-Y. Lien, J.-J. Wu, G.-B. Lee, *Lab Chip* **2011**, *11*, 1521–31.

[8] K.-Y. Lien, C.-J. Liu, P.-L. Kuo, G.-B. Lee, *Anal. Chem.* **2009**, *81*, 4502–9.

[9] H. Tian, A. F. Hühmer, J. P. Landers, *Anal. Biochem.* **2000**, *283*, 175–91.

[10] M. Kokoris, M. Nabavi, C. Lancaster, J. Clemmens, P. Maloney, J. Capadanno, J. Gerdes, C. F. Battrell, *Methods* **2005**, *37*, 114–9.